The Post Christmas Blizzard 26 December 2010

by
Richard H. Grumm
National Weather Service State College, PA 16803

Abstract:

A nor'easter brought heavy snow and blizzard conditions to the East Coast of the United States on 26-27 December 2010. Heavy snow fell from eastern Pennsylvania into eastern New England. Snowfall in portions of northern New Jersey exceeded 3 feet. A wide area received 6 to 20 inches of snowfall. The strong winds, with wind gusts over 60 MPH produced true blizzard conditions across Long Island and southern New England.

With an estimated central pressure of 961 hPa this storm was one of 31 storms with a central pressure lower than 970 hPa since 1958. The strong winds north of the cyclone produced blowing and drifting snow.

From an impacts perspective, the storm disrupted air travel at the end of the busy Christmas weekend. Airlines canceled over 300 flights to and from cities from Baltimore to Boston. Heavy snow caused the National Football League to cancel the game in Philadelphia.

Due to predictability issues, there were many model and ensemble run-to-run inconsistencies or flip-flops. Initial forecasts implied that the storm might miss the major East Coast cities. But subsequent forecasts began to suggest a significant storm for the Mid-Atlantic region and northeast. Ultimately, there was a sharp western edge to the snowfall and the southern extent of the heavy snow fall missed most of the Mid-Atlantic region including Washington, DC and Baltimore, MD. The predictability issues are shown here focusing on the NCEP GEFS forecasts 2-5 days prior to the storm.

1. INTRODUCTION

An East Coast Winter Storm (ECWS) brought snow to the eastern United States from 25-27 December 2010 (Figure 1). The initial wave brought snow to the southeastern United States, as the storm intensified along the coast, heavy snow was observed along the immediate coastal plain from eastern Virginia to southern New England. The heaviest snowfall was over northern New Jersey where several locations received in excess of 20 inches of snowfall.

The storm struck at the end of a busy holiday weekend and thus it had a significant impact on travel along the eastern seaboard. Hundreds of flights into and out of major airports were cancelled. High winds and blowing snow closed roads from New Jersey into southern New England. Clearly, many of the major airports along the coast were closed during the storm. The storm caused the National Football league to postpone the game in Philadelphia leading to a rare Tuesday game.

The track and the pressure pattern associated with the surface cyclone is shown in Figure 2. At 0000 UTC 26 December 2010 the surface cyclone was located off the west coast of Florida in the Gulf of Mexico. The cyclone tracked across Florida and Georgia (Fig. 2b) and moved rapidly up the coast. By 0000 UTC 27 December the central pressure in the Global Forecast System (GFS) analysis was 981 hPa with a -3 standard deviation departure from normal (Fig. 2e). There was a tight pressure gradient north of the surface cyclone. Within this strong pressure gradient strong north-northeasterly winds combined with snowfall produced blizzard conditions from southern New England into New Jersey. The GFS depicted a closed 927 hPa contour at 1200 UTC 27 December off the Coast of Massachusetts. Estimates of the central pressure suggested a 961 hPa cyclone center off the coast of southern New England make this one of the deepest East Coast Cyclones since 1958 (Table 1). Based on re-analysis data there have been 31

storms to reach a central pressure of 970 hPa or lower in the December to March time frame[1].

Full coast ECWS's are not very common during the cold phase of ENSO and are more typically associated with the warm phase of ENSO (DeGaetano et al 2002). Bradbury et al (2003) found a similar trend with more winter storms during the warm phase of ENSO. They found an eastward shift in the storm track with periods of negative NAO. During strongly negative NAO phases the enhanced blocking over Greenland and eastern Canada showed some signal in increase snowfall. The storm of 26-27 December 2010 occurred toward the end of a period of strong high latitude blocking. The NAO ranged from -1.2 to 0.9 from 25-27 December 2010. The MEI was in the -1 to -1.6 range during the month of December.

There was considerably uncertainty related to this storm. Individual models initially showed a storm on or about 25 December along or just off the coast. As the time horizon decreased the storm was forecast to develop later and there was still considerable uncertainty and run-to-run inconsistencies related to when the storm would form and how far west the precipitation shield would extend. By 24 December the models and ensembles appeared to converge on a 26-27 December cyclone, the potential for a deep cyclone, and heavy snowfall. The difficulties along the western edge of the storm were problematic literally to within 24 hours of the storm.

This paper will document the ECWS of 26-27 December 2010. The focus is on the meteorological and climatological significance of this storm from an anomaly perspective. Using the concepts from Hart and Grumm (2001) and Stuart and Grumm (2006) standardized anomalies will be used to show that this storm was and was predicted to a significant winter storm. Ensemble forecasts are presented to show the uncertainty associated with forecasting this high impact winter storm.

2. Methods and Data

The overall pattern was reconstructed using the 00-hour forecasts from the operational GFS. The Japanese Re-analysis data (JRA25:Onagi 2007) was also used to show the pattern and estimate the storm central pressure. The anomalies were derived using the GFS and comparing it to the 30-year mean and standard deviations computed from the NCEP/NCAR re-analysis data (Kalnay et. al 1996). All anomalies herein are shown as standardized anomalies (Hart and Grumm 2001).

The GFS is run on a 27 km grid. However the data shown here is on a 1x1 degree grid. This should mitigate some of the resolution issues between the coarser climatology and the model forecast grids. These effects are normally of minimal impact for parameters above the planetary boundary layer. Some variables such as PW are sensitive and will show higher values in higher resolution models than in the re-analysis dataset.

Forecasts from the NCEP Ensemble Forecast systems (EFSs) will be presented. Standardized anomalies will be presented as described above, computing anomalies from the ensemble mean and the NCEP/NCAR re-analysis data. Probabilities are derived using the ensemble output. These will be raw and uncalibrated probabilities unless specified otherwise.

[1] Analysis from ERA-40 and CFS was conducted by Ryan Maue. Data in Table 1 were produced by with these data but are listed here by lowest pressure so a single event can occur more than once.

For brevity, times will be denoted in the format 26/1200 UTC to signify 1200 UTC 26 December 2010.

3. The Storm system and impacts

i. The pattern and key anomalies

The 500 hPa heights and anomalies in 12-hour increments from 24/0000 through 28/0000 UTC are shown in Figure 3. The key feature at 500 hPa was the short-wave moving under the ridge over central North America. This feature deepened as it moved eastward and the retrograding ridge re-established over western North America. The lower latitude portion of the ridge became progressive (Figs. 3d-i) and the trough deepened rapidly from 25/1200 UTC through 27/1200 UTC (Figs. 3d-3h). Height anomalies of -3 to -4SD were in the closed portion of the trough by 27/1200 UTC. The 250 hPa winds are shown in Figure 4. These data showed a strong subtropical jet (STJ) to the south and a wind maximum coming about the trough. Within the trough the wind anomalies showed weaker than normal winds.

The trough brought a modest surge of moisture into the region (Fig. 5). The precipitable water (PW) in the warm sector showed 20-35 mm of PW with 1 to 2 SD PW anomalies. Relative to the heavy rain storm along the West Coast 16-21 December 2010, this events PW anomalies were minimal.

Similar to previous heavy rain events (Grumm and Hart 2001) and heavy snow events (Stuart and Grumm 2006) this storm had a strong low-level jet with the heavy snow bands forming within this feature (Figure 6). North of the surface and 850 hPa cyclones (Figs. 2 & 6) there were strong northeasterly winds at 850 hPa. A broad area of -3 to -5SD easterly wind anomalies developed by 26/1800 UTC (Fig. 6c) with embedded -5 to -6 an event -6SD u-wind anomalies (Fig. 6d) at 27/0000 UTC. Near the nose of this feature snowfall amounts of over 20 inches were observed in New York City and New Jersey. Video evidence[2] suggests that over 36 inches of snow fell in at least one location in New Jersey. The 850 hPa winds and total wind anomalies (Fig. 7) suggest that the blizzard conditions likely occurred in areas where the total wind anomalies were 3 to 5SDs above normal (Fig. 7e-g).

ii. Precipitation and observations

The snowfall associated with the event was shown in Figure 1. The insets showed the two general areas of heavy snowfall in the New York Metropolitan area and southern New England. The red points in New Jersey saw snowfall in excess of 20 inches. The water equivalent associated with the snowfall is shown in Figure 8. These data suggest over 16 mm of precipitation fell over coastal New Jersey, the Hudson Valley of New York, and Long Island, New York. Maine and New Hampshire had over 16 mm of precipitation as did the Boston area. These data suggest over 32 mm of precipitation near and south of Boston. Due to the storm track (Fig. 2) and the surge of warm air near the

[2] CNN news story with video iReporter too images every 5-minutes for 20 hours recording a yard stick getting buried in Belmar, NJ. http://www.cnn.com/video/#/video/ireports/2010/12/27/irpt.captures.rare.snowfall.cnn?hpt=C2

low center, not all the precipitation in Massachusetts fell as snow. These data likely missed the mesoscale detail that produced the 20 to 30 inches of snowfall in New Jersey.

In addition to the snow, the storm produced strong winds. A listing of the observations at Islip, New York is shown in Table 2. These data show over 8 hours of strong winds with sustained winds of 20 to 30KTS and wind gusts over 50KTS. There was a prolonged period of 1/8 to ½ mile visibilities at this site. Other sites examined, such as LaGuardia indicated that these strong winds, heavy snow and reduced visibilities were common in the New York Metropolitan area. With winds and gusts over 35 mph and visibilities under ¼ mile for over 3 hours, this storm clearly was a blizzard across portions of New Jersey, southern New York and southeast Connecticut.

The upper panel of Figure 8 shows the total precipitation associated with the storm system. The storm produced precipitation along and north of the cyclone track (Fig. 2) from east Texas to northern Florida and up the coast. In the southern States, the precipitation was streaky and suggest the convergence of two waves as there was snow in the Tennessee and Ohio Valleys with the northern wave. Once the two waves merged and the single cyclone evolved along the coast, there was a sharp western edge to the precipitation. Forecasting this sharp edge was the difficult task associated with this high impact winter storm.

iii. Forecasts-long-range

NCEP GEFS forecasts of mean sea-level pressure and anomalies from 18-20 December 2010 valid at 1200 UTC 26 December 2010 are shown in Figure 9. These ensemble mean data showed a cyclone off the East Coast and likely too far east to be produce significant impact to the coastal regions outside of easternmost New England. This storm was fast relative to subsequent forecasts and implied a storm over the Tennessee Valley on Christmas Eve then along the Carolina Coast by Christmas morning (not shown).

Figure 10 shows the forecasts valid at 27/0000 UTC from a shorter set of GEFS forecasts. The time was moved due to the change in the timing of the storm evolution. Though many of these ensemble mean forecasts showed a deep cyclone, most were well offshore. However the shorter range forecasts (Figs. 9i-g) showed a sharp westward shift to the cyclone track. Though not shown, the larger anomalies and generally deeper cyclone were due in part to smaller spread between members.

Figure 11 moves the cyclone forecasts forward another day. Not visible in the single images is that the track of the cyclone in the most recent 3 forecast cycles showed the primary cyclone coming out of the Gulf of Mexico, well south of earlier forecasts. Additionally, the location and intensity of the cyclone along the East Coast by 27/0000 UTC varied considerably which impacted the precipitation shields western extent (not shown).

Figure 12 shows the two additional GEFS cycles from 24 December, both the 24/1200 and 24/1800 UTC forecasts showed a deeper cyclone and a cyclone track well west of previous cycles. ***These forecasts represented a significant westward shift of the cyclone track relative to previous forecasts***. There was a sudden convergence of forecasts toward a deeper and more westward tracking cyclone. These forecasts depicted a close cyclone moving across the northern Gulf of Mexico, across northern Florida and

up the East Coast (not shown). This shift had dramatic impact on the potential snow and precipitation shield north and west of the cyclone center. This shift was clearly visible in the NCEP SREF (Fig. 13) and in forecasts from other modeling centers deterministic and ensemble forecasts (Fig. 14).

iv. Cyclone tracks

The cyclone tracks from 4 successive cycles are shown in Figure 14. These data clearly show the predictability issues associated with this cyclone. The forecasts from 24/0000 UTC (Fig. 14a) showed that *the verifying cyclone (cyan color) was west of all the forecasts* until the cyclone got north of 40N. Additionally, the verifying cyclone was west of the 40N 70W benchmark often used for winter storms while *all the model and ensemble mean guidance showed the cyclone tracking to the east of this point*. These forecasts implied a near miss for the East Coast as all forecasts were east of the verifying cyclone position.

Forecasts issued 12 hours later are shown in Figure 14b showed that the GFS (green) and the GEFS (dark green) jogged the cyclone westward, close to the verifying track. From the southeast coastal regions to off the coast of Maine, the GFS and GEFS clearly verified better than all other guidance. However, forecasters in the Canadian Maritimes likely would have been better served by the ECMWF.

Moving forward to 24/1800 UTC (Fig. 14c), with the exception of the ECWF and the CMC all models showed a continued jog of the cyclone track to the west. The GFS forecasts likely verified poorly once the cyclone reached 40N as it then tracked it to the west. By 25/0000 UTC all but the 1200 UTC EC jogged the cyclone westward and all appeared to align well with the verification. The GFS still had problems once the cyclone moved north of 40N.

These data clearly show marked issues related to predictability. The slow alignment of the forecasts and the jog of the cyclone track to the west with time suggest that model initialization issues may have played a role in the forecast errors. These tracks would have and did shift the precipitation shield associated with the storm westward with time.

v. Uncertainty issues

All models and ensembles showed uncertainty issues with the cyclone track. This impacted the western extent of the precipitation shield. For brevity cycle comparisons of the GFS are shown here. Data will show the forecast of the parameter with the error based on the verifying GFS analysis, computed as forecast minus observed.

Figure 15 depicts the 500 hPa heights and errors from 9 GFS cycles valid at 27/0000 UTC. Images for each 6-hour period were produced but are not shown. The older forecasts initialized at 23/1800 through 24/0600 UTC show large height errors in the trough over the southeastern United States. These errors become significantly smaller with the 24/1200 UTC GFS cycle (Figure 15d), errors decrease with time thereafter.

The corresponding mean-sea level pressure with errors is shown in Figure 16. These data show large pressure errors north of the forecast cyclone position which drop precipitously by 24/1200 UTC (Fig. 16d) and continue to drop as forecast length decreases. Large negative errors on the west side of the cyclone after 24/1200 UTC imply forecast pressure values were lower than observed values especially in the Mid-Atlantic region. Even as the forecasts moved the cyclone closer to the coast they still contained significant errors. However, the earlier cyclone tracks to the east produced large positive errors from the Mid-Atlantic region into New England from forecasts initialized from 23/1800 through 24/0600 UTC.

Figure 17 shows successive forecasts in 6-hour increments of the surface cyclone evolution from the 24/1200 UTC GFS. These data show relatively small errors as the cyclone moved out of the Gulf of Mexico and up the coast. The errors grew rapidly during the period of forecast rapid cyclogenesis between 26/1800 and 27/0600 UTC. A robust ensemble forecast system would likely show large spread in the same areas where the forecast errors are large indicating the uncertainties related to cyclogenesis. The errors associated with the 24/1200 UTC were smaller than those associated with the previous 24/0000 and 24/0600 UTC cycles which had large positive errors north of the cyclone center (Fig. 18). The 24/0600 UTC GFS had large positive pressure errors from the eastern Gulf up the East Coast.

Figure 19 shows the traditional ensemble plots from the NCEP GEFS. The left images correspond to the cycle time in Figure 17. Due to convergence of the GEFS forecasts, based on the GFS, a deep cyclone was predicted south of Long Island, NY. The largest spread 4-8 hPa was north and west of the cyclone position. It lacked the sharpness depicted in the GFS forecast valid at 27/0600 UTC (Fig. 17h) but the GEFS clearly depicted the low confidence forecast regions implied and verified in the GFS error field.

vi. Forecasts-short-range

Examine the impacts on the QPF and subsequent snowfall. Sharp edges to this storm. Need 9 panels for a full cycle not 9 cycles.

4. Conclusions

A high impact winter storm brought heavy snow from eastern Delaware into eastern New England. North of the surface cyclone a strong and highly anomalous LLJ developed. This feature brought strong winds and wind gusts over 45KTS to southern New England, Long Island, and northern New Jersey. True blizzard conditions, with over 10 hours of strong winds and visibilities under ¼ statue mile were common in the blizzard area. The strong gradient was associated with a deep cyclone, one of only 31 cyclones since 1958 to have a central pressure below 970 hPa. This high impact storm closed airports and roads at the end of a busy holiday weekend. The NFL was forced to postpone the scheduled game in Philadelphia due to the heavy snowfall.

This storm and its impact were difficult to predict. Forecasts from global forecast models and global ensemble forecast systems suggested the potential for a significant cyclone along or just off the coast at least 7 days in advance. However, there was

considerable uncertainty as to how close to the coast this storm would track. The uncertainty with this storm remained high to within 18-30 hours of the onset of heavy snowfall. There were indications that trough merger processes (Bosart and Gaza 1990) played a significant role uncertainty issues with this cyclone. The relatively short lead time created problems for those forced to deal the potential heavy snow and eventually, the blizzard conditions associated with this winter storm.

The NCEP cyclone track forecasts (Fig. 14) and the GEFS and SREF ensemble mean data suggest that confidence in the forecasts increased dramatically after 24/1200 UTC. The tracks of the forecasts issued prior to 24/1200 UTC were all east of the verifying analysis but some were within the envelope of solutions after 24/1200 UTC. This dramatic shift is not explained here but it is a worthy course of study to learn what caused this shift and how this information could be used to improve future forecasts. It is possible that some portion of the errors were related to model initializations as different models and ensemble forecast systems responded and converged toward more accurate cyclone track forecasts at different times. Tests of different models with other centers initial conditions could provide insights into this issue. Reductionist testing may provide some useful insights and thus improve future simulations of this event. However, the nature of chaos and predictability will likely produce future events of similar difficulty. Unlike the surprise winter storm of 25 January 2000 (Zhang et al. 2003), this storm and its potential magnitude relatively well predicted though the track and precipitation shield were poorly predicted. As shown in Figure 14, the verifying cyclone was west of and thus outside the envelope of solutions of all prediction centers forecasts at several forecast initialization cycles. The differences in the cyclone forecast tracks between models and the resulting forecast errors likely relate back to a combination of synoptic and mesoscale issues, as suggested by Zhang et al. (2003). Rapid error growth at mesoscales (Ehrendorfer 1999) likely contributed to both errors and differences between various models. Studies of varying initial conditions will likely provide insights as to model initialization and synoptic scale issues. Studies with model resolution and moist convective and other mesoscale processes will likely shed some light on the impacts of the problem with this cyclone. Ultimately, as stated by Zhang et al. 2003: "*the growth of small-scale differences clearly imposes an upper bound on the predictability of the flow, much as foreseen by Lorenz (1969).*" And thus, this event and the associated errors may not be unique and we will encounter similar errors in the future.

The errors in the GFS (Figs.15-18) showed that there was a marked decrease in both the 500 hPa height and mean-sea level pressure errors from forecasts initialized on and after 1200 UTC 25 December 2010. The cyclone track data (Fig. 14) also showed a shift in all the guidance after 24 December 2010. This posses an intriguing question as to what caused a dramatic decrease in position errors of the cyclone, pressure errors in the cyclone, and errors in the 500 hPa height field. Clearly, all the models and thus the EFS's were sensitive to this issue. The predictability horizon with this high impact winter storm was relatively short due to the uncertainty.

On a positive note, the overall error patterns in the GFS appeared to match the spread in the NCEP GEFS. This implies that the GEFS contained the correct uncertainty information as the spread remained relatively high in regions where the single GFS had its largest errors. It would appear that in cases of rapid cyclogenesis one has to leverage and accept the limits of predictability.

In addition to the uncertainty and confidence issues associated with this storm are the issues related to a full coast storm during a La Nina year. Full coast storms tracking out of the Gulf of Mexico are relatively common in El Nino years and rare during La Nina winters (DeGaetano et al. 2002). This storm clearly was a full coast storm. It is possible that the retrograding high latitude block, associated with a strongly negative NAO, caused a westward shift in the storm track (Bradbury et al 2003) and thus produced conditions favoring a full coast storm during a La Nina winter.

5. Acknowledgements

Special thanks for the Albany maproom for dialog on forecasts of the storm and summary information related to the storm. Member Ryan Maue provided the historical data on recent deep cyclones along the East Coast. The Stony Brook CSTAR list provide insights relative to uncertainty issues. The NCEP HPC, Dan Peterson and Marty Rausch provided storm track images (Fig. 14) and insights into trough merger issues used within. A special thanks to Josh Korotky for insights on reductionism and the limits of predictability, as he stated "*ultimately reductionists cannot truly appreciated the view from outside the forest.*"

6. References

Bradbury, J.A, Keim, B.D and C. P Wake, 2003: The Influence of Regional Storm Tracking and Teleconnections on Winter Precipitation in the Northeastern United States. Annals of the Association of American Geographers, 93(3), 2003, pp. 544–556.

DeGaetano, A. T., M. E. Hirsch, and S. J. Colucci. 2002.Statistical prediction of seasonal East Coast winter storm frequency. Journal of Climate 15:1101–17.

Ehrendorfer, M., R. M. Errico, and K. D. Raeder, 1999: Singular vector perturbation growth in a primitive equation model with moist physics. *J. Atmos. Sci.,* **56,** 1627–1648.

Gaza, B. and L. F. Bosart, 1990: Trough merger characteristics over North America. *Wea. Forecasting,* **5**:314–331.

Graham, Randall A., Richard H. Grumm, 2010: Utilizing Normalized Anomalies to Assess Synoptic-Scale Weather Events in the Western United States. Wea. Forecasting, 25, 428-445.

Grumm, R.H. and R. Hart. 2001: **Standardized** Anomalies Applied to Significant Cold Season Weather Events: Preliminary Findings. *Wea. and Fore.***, 16,736**–754.

Hart, R. E., and R. H. Grumm, 2001: Using normalized climatological anomalies to rank synoptic scale events objectively. *Mon. Wea. Rev.*, **129,** 2426–2442.

Lorenz, E. N., 1969: The predictability of a flow which possesses many scales of motion. *Tellus,* **21,** 289–307.

Stuart N. A., and R. H. Grumm, 2006: Using wind anomalies to forecast east coast winter storms. *Wea. and Forecasting,* **21**, 952-968.

Onogi, K., J. Tsutsui, H. Koide, M. Sakamoto, S. Kobayashi, H. Hatsushika, T. Matsumoto, N. Yamazaki, H. Kamahori, K. Takahashi, S. Kadokura, K. Wada, K. Kato, R. Oyama, T. Ose, N. Mannoji and R. Taira (2007) : The JRA-25 Reanalysis. J. Meteor. Soc. Japan, 85, 369- 432.

Zhang,F, C. Snyder,R.Rotunno, 2003: Effects of Moist Convection on Mesoscale Predictability. JAS,60,1173-1185.

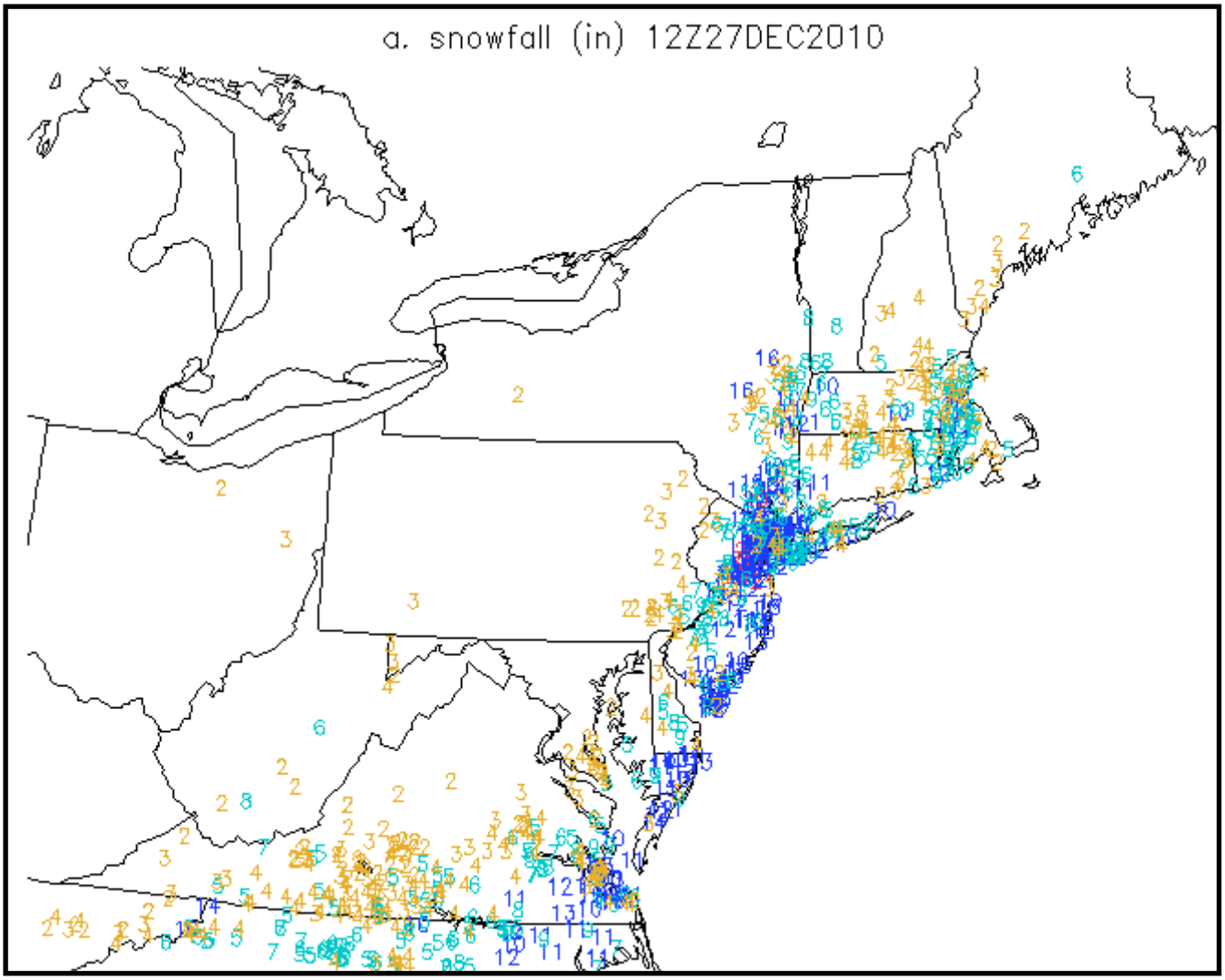

Figure 1. Snow fall (inches) from public information statements valid as of 1200 UTC 27 December 2010. Yellow shows 2-5 inches, cyan shows 5-10 inches, blue shows 10-20 inches and red shows over 30 inches of snowfall. Return to text.

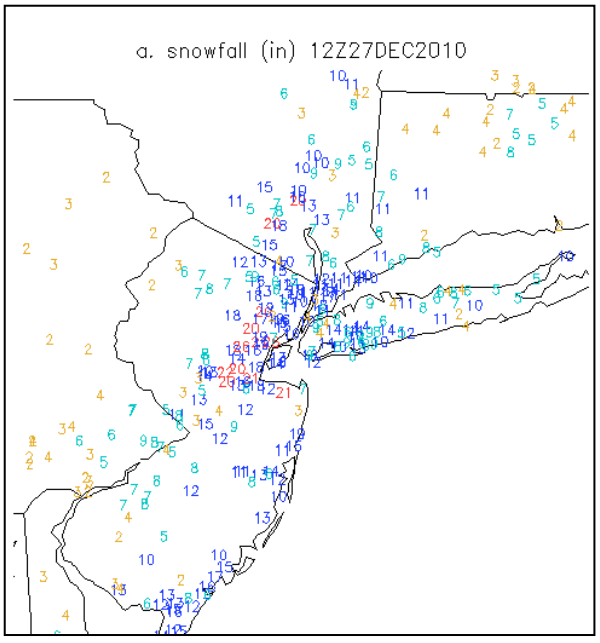

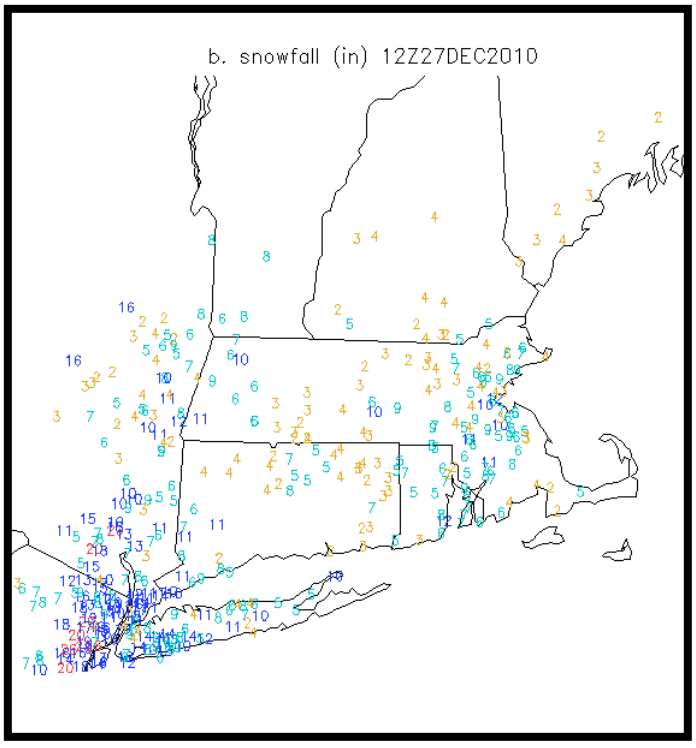

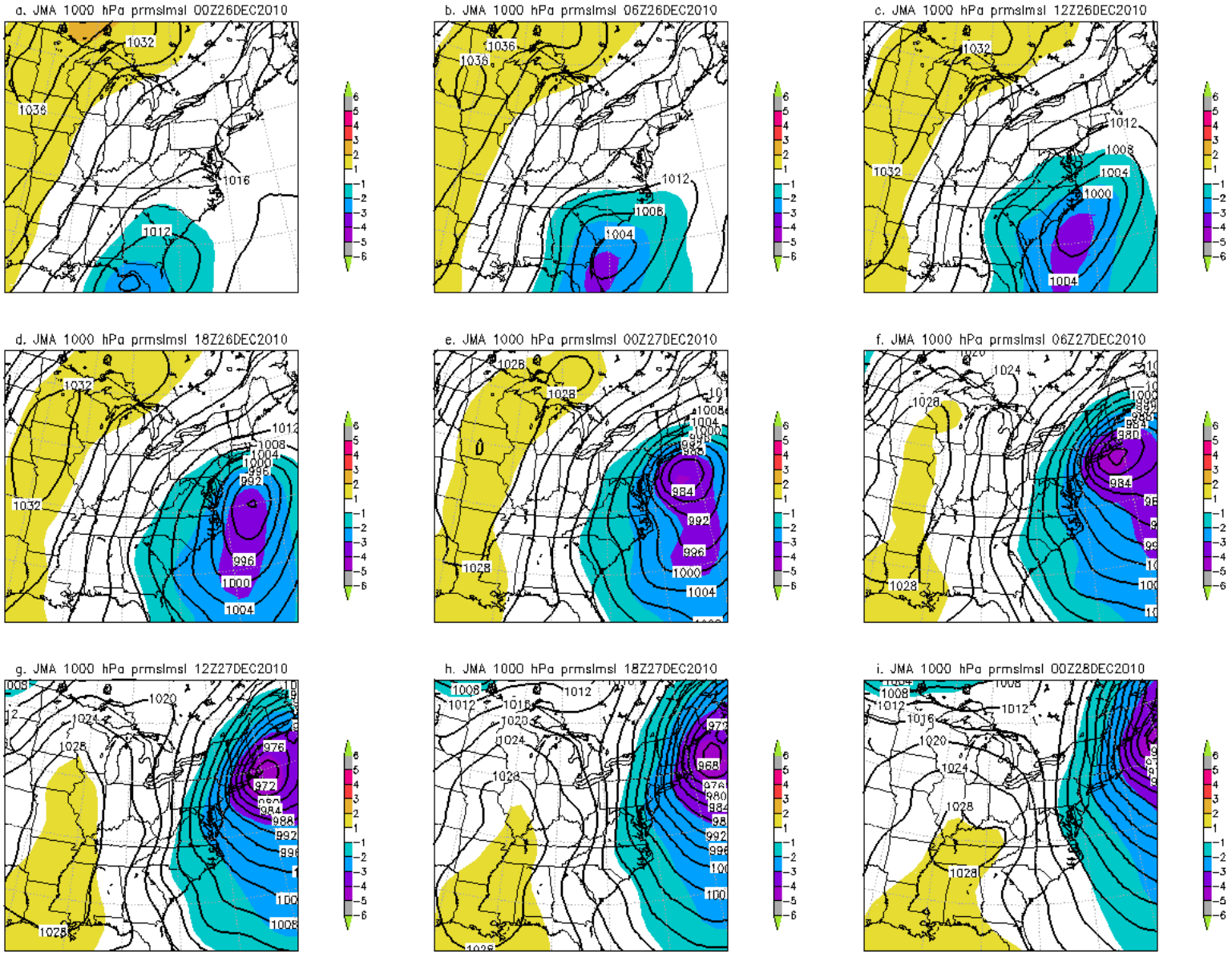

Figure 2. GFS 00-hour forecasts of mean sea-level pressure (hPa) and standardized anomalies (standard deviations from normal) for the 9 6-hour periods from a) 0000 UTC 26 December 2010 through i) 0000 UTC 28 December 2010. Return to Text.

Date	Central Pressure (hPa)
00Z08MAR1969	955.242
18Z17MAR1981	957.297
12Z21JAN2000	957.928
00Z27DEC1970	959.528
12Z17MAR1981	960.538
12Z26JAN1978	960.842
18Z07MAR1969	960.972
18Z26JAN1978	961.999
18Z21JAN2000	962.076
00Z18MAR1981	962.281
18Z26DEC1970	963.017
18Z02FEB1976	963.037
12Z05FEB1995	963.64
06Z09MAR2005	963.687
00Z14JAN2002	963.817
18Z01DEC1964	963.904
00Z21JAN1961	963.911
00Z02DEC1964	964.716
12Z04JAN1989	964.911
06Z02MAR1968	965.001
06Z14MAR1993	965.036
12Z10MAR1969	965.426
12Z14MAR1993	965.608
18Z04MAR1971	965.631
00Z02MAR1968	965.706
00Z14MAR1993	965.959
06Z21JAN2000	966.289
00Z05MAR1971	966.309
00Z18FEB1974	966.389
12Z15JAN1982	966.53
06Z12JAN1987	966.552
18Z01MAR1968	966.562
12Z02MAR1968	966.711
18Z29JAN1979	966.842

Table 1. Dates of sub-970 hPa pressures (hPa) from ERA-40 reanalysis (1958-1979) and the new NCEP CFSR reanalysis (1979-2009), and looking in a box bounded by 30-45N and 80-65W for the lowest analyzed MSLP during December – March. *Data courtesy of Ryan Maue.* Return to text.

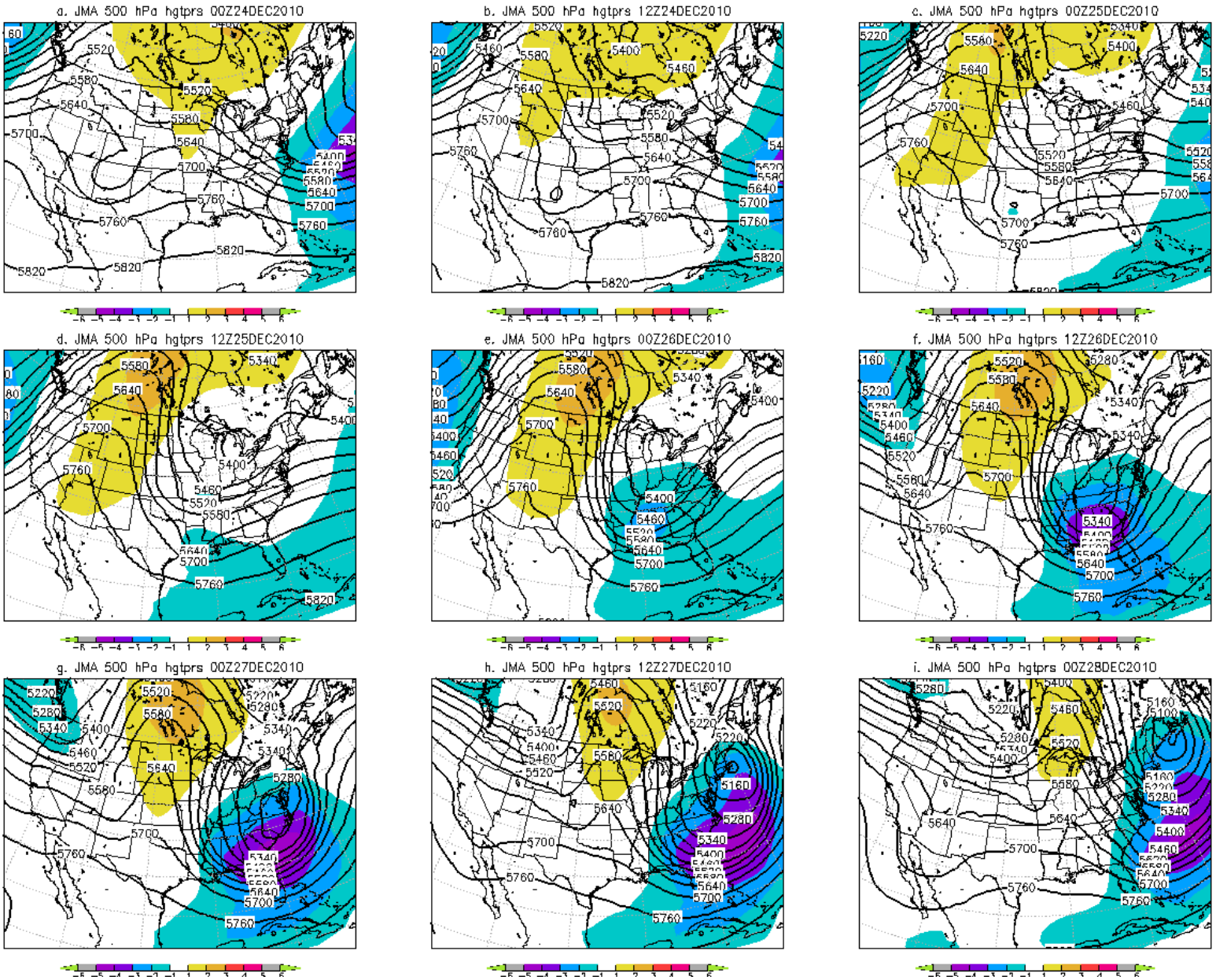

Figure 3. As in Figure 2 except for 500 hPa heights and anomalies in 12-hour increments from a) 0000 UTC 24 December 2010 through i) 0000 UTC 28 December 2010. Return to text.

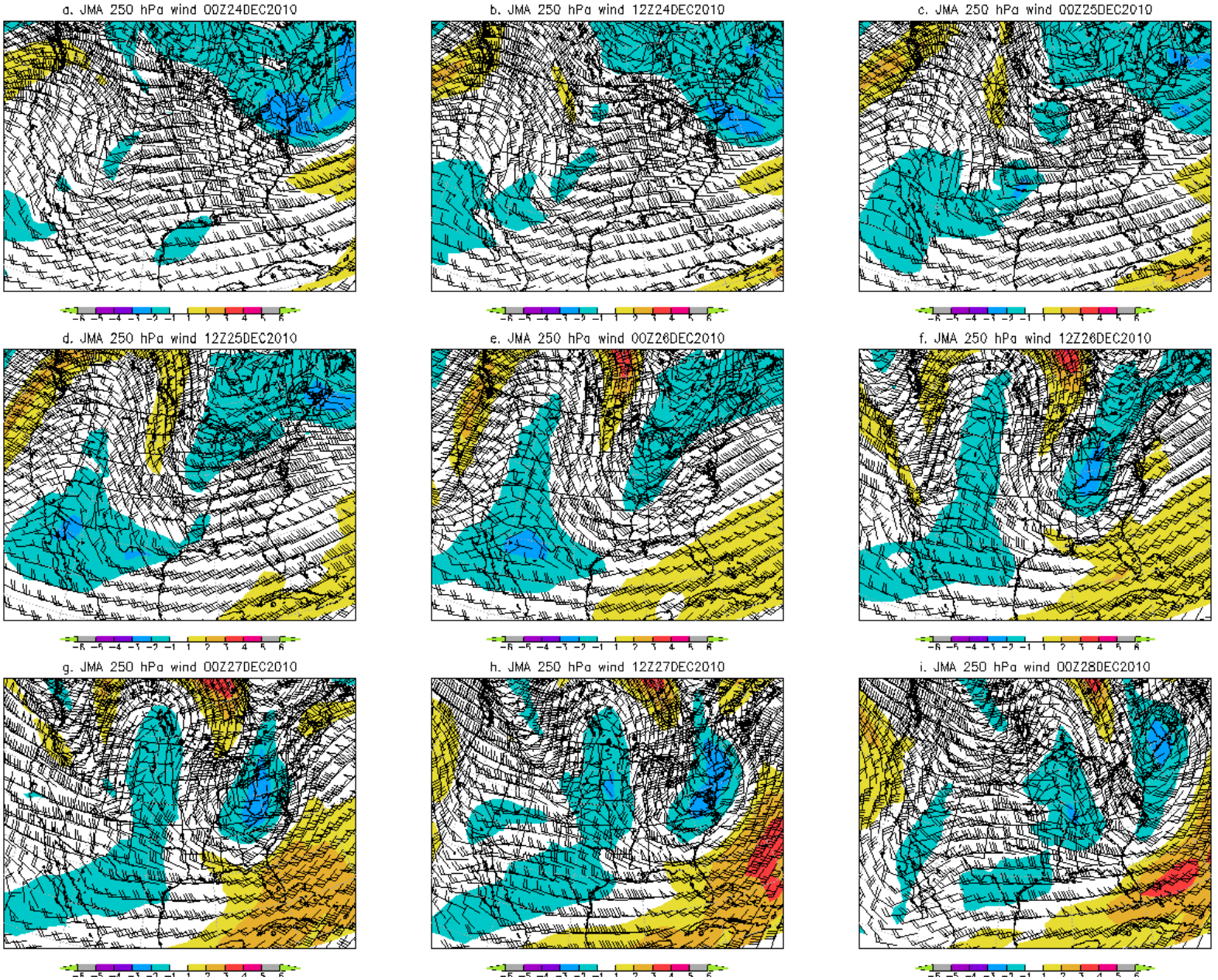

Figure 4. As in Figure 3 except for 250 hPa winds (ms-1) and total wind anomalies. Return to text.

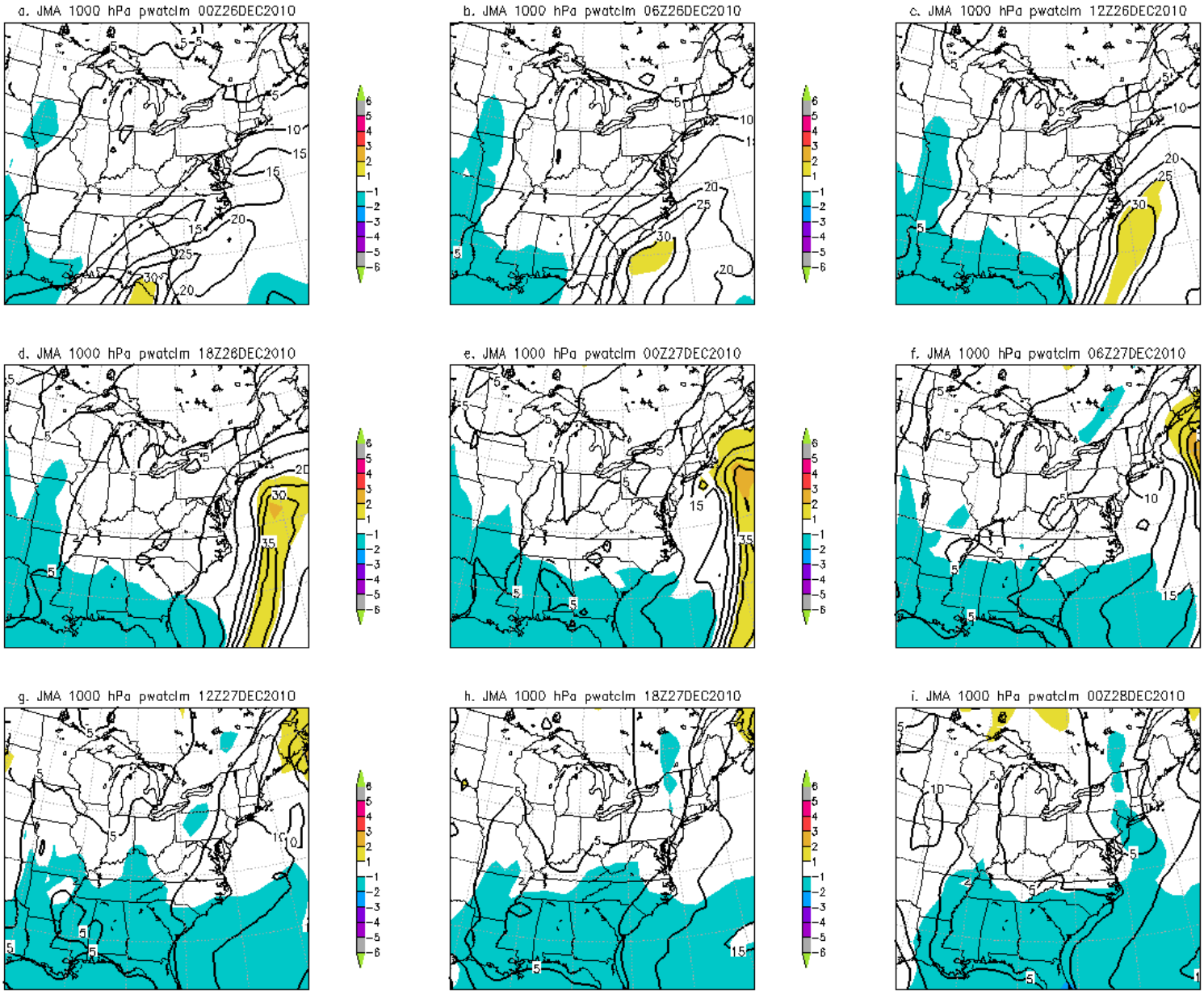

Figure 5. As in Figure 2 except for precipitable water (mm) and precipitable water anomalies. Return to text.

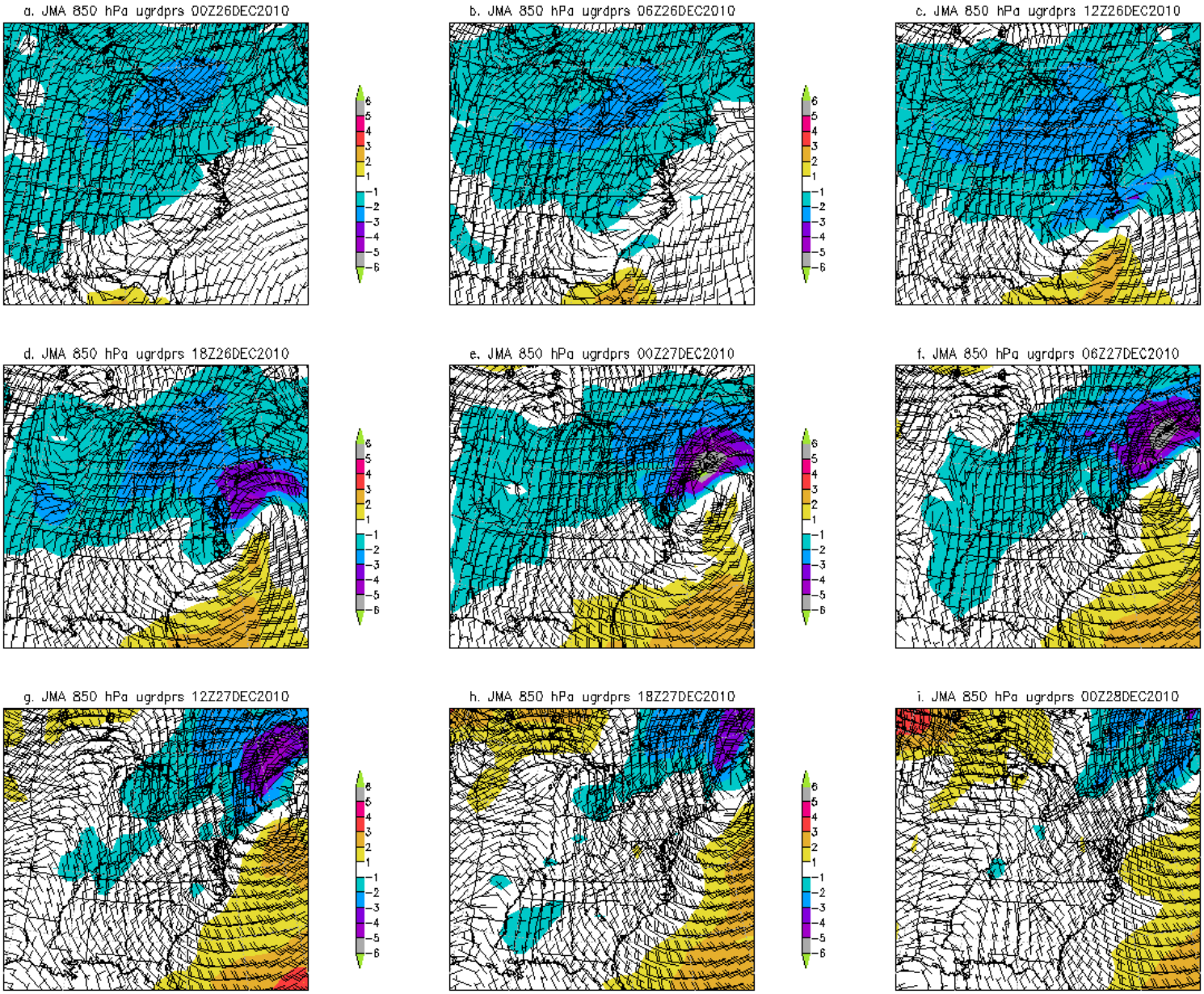

Figure 6. As in Figure 4 except for 850 hPa winds and u-wind anomalies. Return to text.

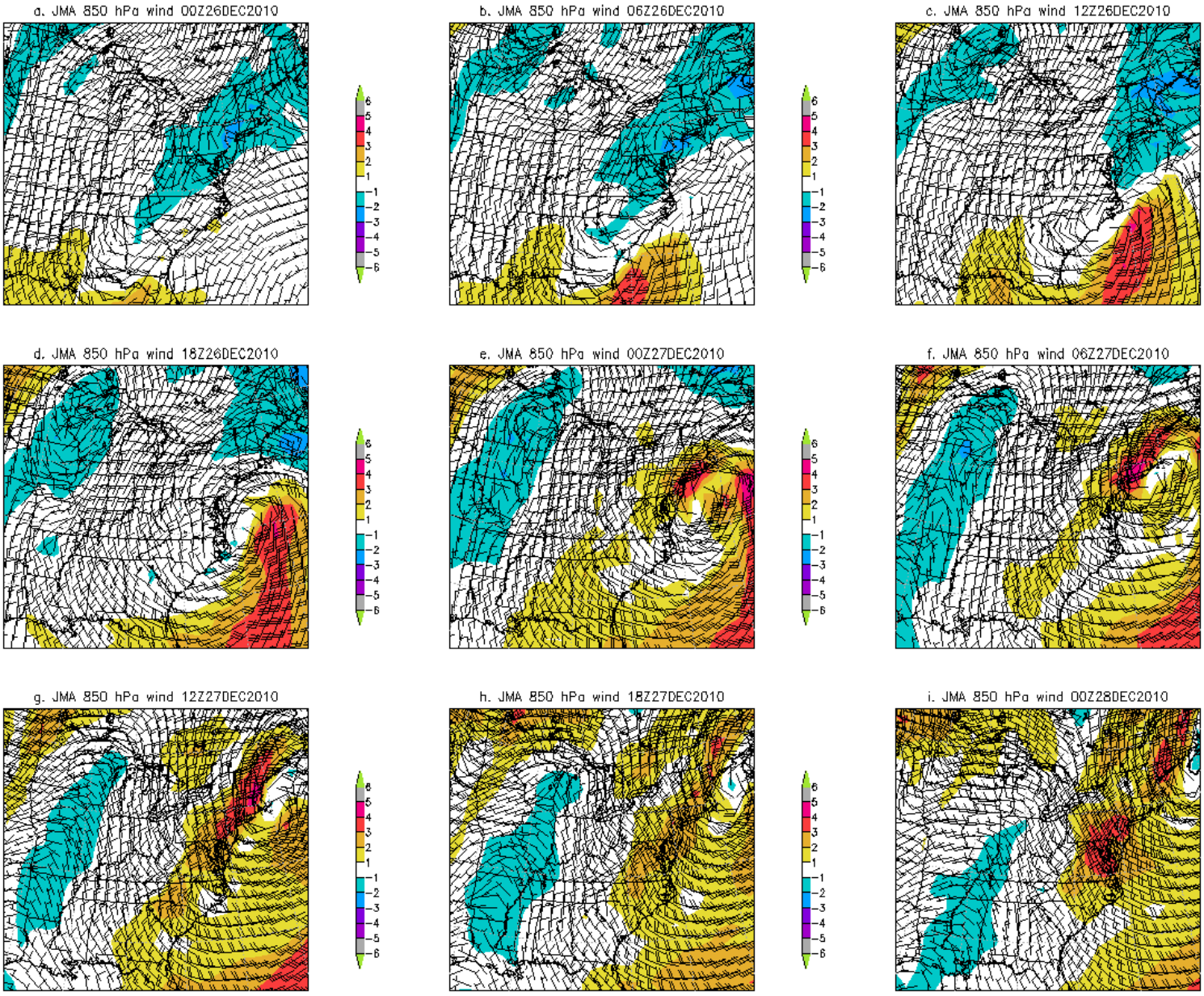

Figure 7. As in Figure 6 except for 850 hPa winds and total wind anomalies. Return to text.

KISP Observations:

```
METAR KISP 261756Z 03020G25KT 1/2SM R06/2600V4000FT SN SCT005 OVC009 M01/M04 A2963 RMK
AO2 SLP035 4/001 P0003 60005 T10111044 11011 21022 58063
SPECI KISP 261840Z 03018G24KT 1/2SM R06/2000V2200FT SN FZFG SCT002 BKN008 OVC013 M01/M04
A2958 RMK AO2 PK WND 03026/1819 P0003
METAR KISP 261856Z 03020G25KT 1/2SM R06/2400V3000FT SN FZFG SCT002 OVC008 M01/M04 A2957
RMK AO2 PK WND 03027/1844 SLP014 SNINCR 1/2 P0005 T10111039
METAR KISP 261956Z 02022G30KT 1/4SM R06/2000V2600FT SN FZFG SCT002 OVC008 M02/M04 A2949
RMK AO2 PK WND 03032/1946 SLP987 P0003 T10221044
SPECI KISP 262003Z 02024G31KT 1/4SM R06/2000V2400FT +SN FZFG BKN002 OVC008 M02/M05 A2948
RMK AO2 PK WND 03031/2003 P0000
METAR KISP 262056Z 01026G34KT 1/4SM R06/2000V3000FT +SN FZFG BKN003 OVC008 M03/M06 A2939
RMK AO2 PK WND 03034/2055 PRESFR SLP952 SNINCR 1/3 P0003 60011 T10281056 58083
SPECI KISP 262130Z 01025G35KT 1/4SM R06/2000V2800FT +SN FZFG VV001 M03/M06 A2937 RMK AO2
PK WND 02038/2106 P0000 $
SPECI KISP 262142Z 36024G34KT 1/4SM R06/2000V2800FT +SNPL FZFG VV001 M03/M06 A2937 RMK
AO2 PK WND 02038/2106 PLB41 P0002 $
METAR KISP 262156Z 01026G39KT 1/4SM R06/2000V2600FT +SNPL FZFG VV001 M03/M06 A2935 RMK
AO2 PK WND 35039/2152 PLB41 SLP941 SNINCR 1/4 P0002 T10331061 $
METAR KISP 262256Z 36029G40KT 1/4SM R06/2200V2800FT SNPL FZFG BLSN VV001 M03/M06 A2929
RMK AO2 PK WND 35040/2256 PRESFR SLP920 SNINCR 1/5 P0004 T10331061 $
SPECI KISP 262317Z 01024G38KT 1/4SM R06/3000V4500FT +SN FZFG BLSN BKN001 OVC011 M03/M06
A2929 RMK AO2 PK WND 01038/2315 PLE16 P0002 $
METAR KISP 262356Z 01032G44KT 1/4SM R06/2800V4000FT SN FZFG BLSN BKN001 OVC013 M03/M06
A2923 RMK AO2 PK WND 36047/2324 PLE16 PRESFR SLP900 SNINCR 1/6 4/006 P0004 60021
T10331061 11011 21039 58052 $
SPECI KISP 270011Z 36038G47KT 1/4SM R06/2800V4500FT SNPL FZFG BLSN BKN001 OVC013 M03/M06
A2919 RMK AO2 PK WND 36047/0011 PLB11 PRESFR P0000 $
SPECI KISP 270031Z 36021G43KT 1/4SM R06/2800V4500FT +SN FZFG BLSN VV001 M03/M06 A2919 RMK
AO2 PK WND 36047/0011 PLB11E31 P0002 $
METAR KISP 270056Z 02032G50KT 1/8SM R06/2400V4000FT +SN FZFG BLSN BKN001 OVC013 M03/M05
A2916 RMK AO2 PK WND 03050/0055 PLB11E31 SLP876 SNINCR 1/7 P0003 T10281050 $
SPECI KISP 270120Z 36034G47KT 1/8SM R06/1200V2000FT +SN FZFG BLSN BKN001 OVC011 M03/M05
A2911 RMK AO2 PK WND 01047/0120 PRESFR P0002 $
SPECI KISP 270140Z 36037G52KT 1/8SM R06/1800V2600FT +SN FZFG BLSN VV001 M03/M05 A2907 RMK
AO2 PK WND 01052/0138 PRESFR P0002 $
METAR KISP 270156Z 01035G49KT 1/4SM R06/1800V3000FT +SN FZFG BLSN VV001 M02/M05 A2906 RMK
AO2 PK WND 01052/0138 SLP843 SNINCR 2/9 P0002 T10221050 $
METAR KISP 270256Z 01033G44KT 1/4SM R06/2800V4500FT SN FZFG BLSN BKN001 BKN004 OVC014
M03/M05 A2900 RMK AO2 PK WND 36056/0210 SLP823 SNINCR 1/10 P0002 60007 T10281050 56077 $
METAR KISP 270356Z 01035KT 1/8SM R06/2600V5000FT SN FZFG BLSN BKN001 BKN004 OVC010
M03/M05 A2896 RMK AO2 SLP809 SNINCR 1/11 P0000 T10281050 $
METAR KISP 270456Z 02035KT 1/4SM R06/2200V2600FT SN FZFG BLSN BKN001 BKN004 OVC010
M03/M05 A2896 RMK AO2 SLP807 T10281050 401001039 PNO $
SPECI KISP 270527Z 02035KT 1/8SM R06/1600V2200FT SN FZFG BLSN VV001 M03/M05 A2895 RMK AO2
PNO $
SPECI KISP 270546Z 02035KT 1/8SM R06/1400V2400FT SN FZFG BLSN VV001 M03/M05 A2894 RMK AO2
PNO $
METAR KISP 270556Z 02030KT 1/8SM R06/1400V2000FT SN FZFG BLSN VV001 M05/M05 A2894 RMK AO2
SLP802 4/012 6//// T10501050 11022 21050 56021 PNO $
SPECI KISP 270628Z 02030KT 1/8SM R06/1800V2400FT SN FZFG BLSN VV001 M05/M06 A2895 RMK AO2
PNO $
METAR KISP 270656Z 02035KT 1/4SM R06/2000V2800FT SN FZFG BLSN VV002 M06/M07 A2896 RMK AO2
SLP809 T10601070 PNO $
METAR KISP 270756Z 02035KT 1/4SM R06/2000V2600FT SN FZFG BLSN VV001 M06/M07 A2896 RMK AO2
SLP809 T10611072 PNO $
SPECI KISP 270837Z 02035KT 1/4SM R06/1800V2000FT SN FZFG BLSN VV001 M06/M07 A2898 RMK AO2
PNO $
SPECI KISP 270846Z 02035KT 1/4SM R06/2000V3000FT SN FZFG BLSN VV001 M06/M07 A2898 RMK AO2
PNO $
```

Table 2. Observations at Islip, New York from 1756 UTC 26 December through 0846 UTC 27 December 2010. Return to text.

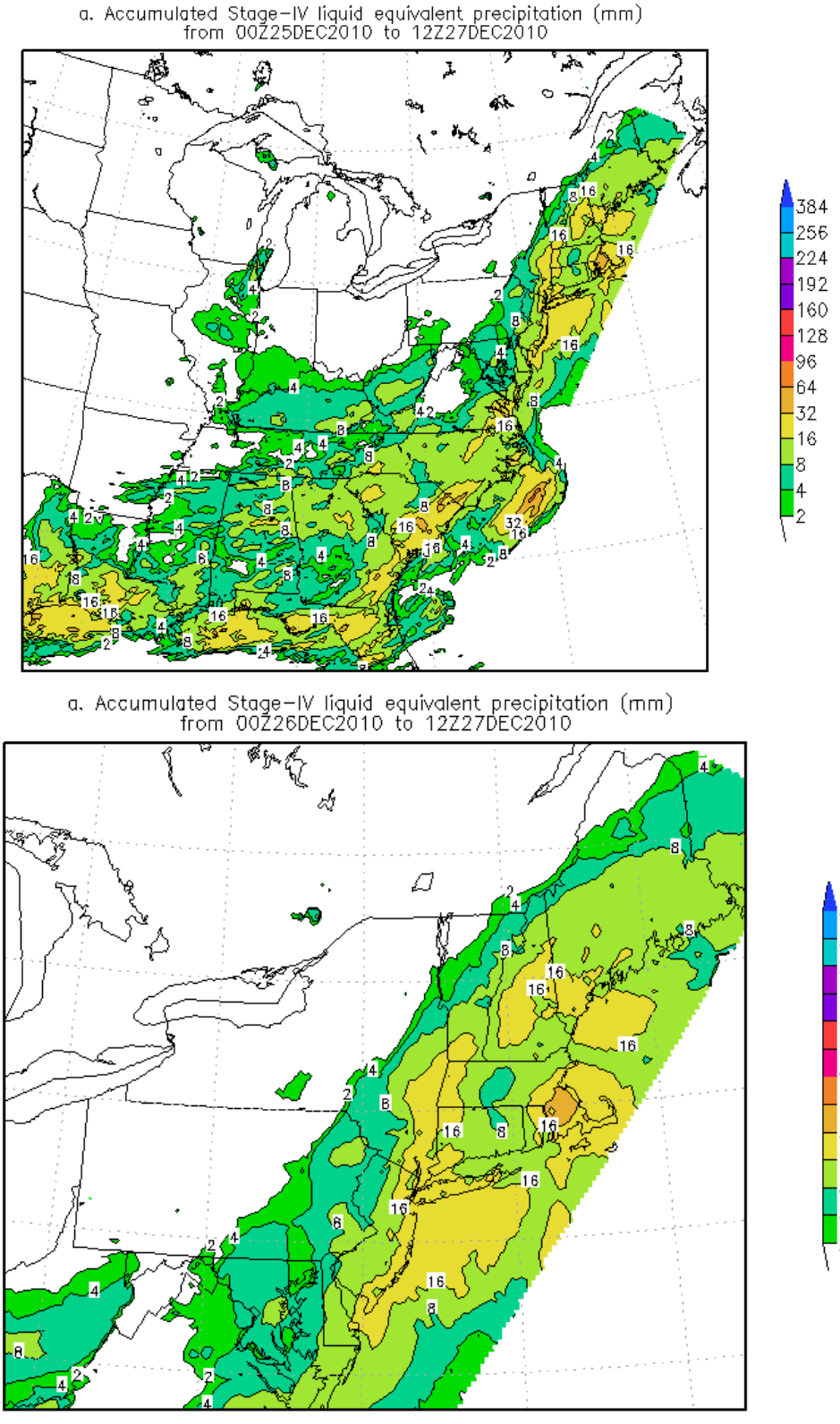

Figure 8. Stage-IV precipitation data (mm) showing total observed liquid equivalent precipitation from (top) 0000 UTC 25 December through 1200 UTC 27 December 2010 and (bottom) 0000 UTC 25 to 1200 UTC 27 December 2010. Return to text.

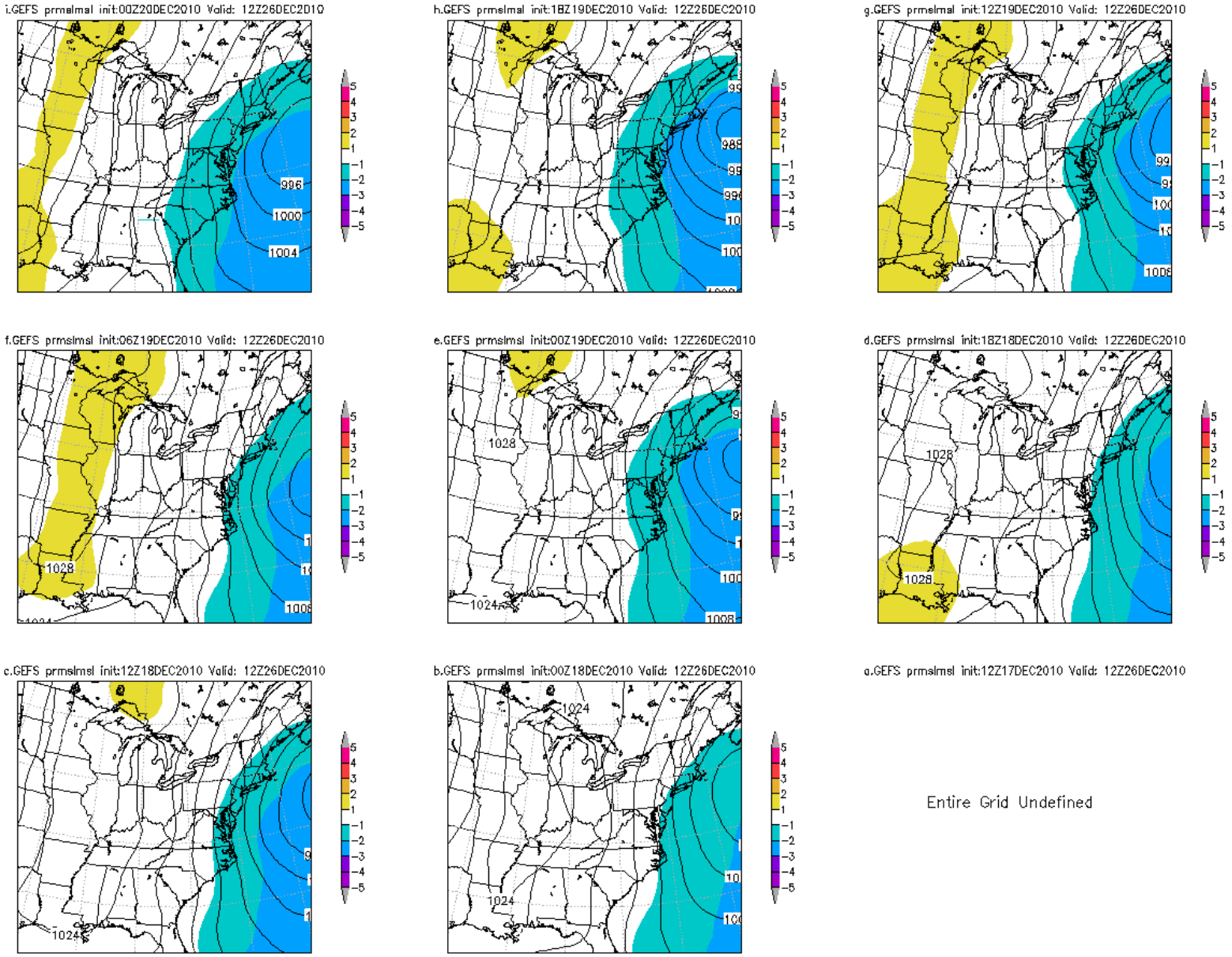

Figure 9. NCEP GEFS forecasts of mean sea level pressure (hPa) and pressure anomalies valid at 1200 UTC 26 December 2010 from forecasts initialized at i) 0000 UTC 20 December 2010, h) 1800 UTC 19 December 2010, g) 1200 UTC 19 December 2010, f) 0600 UTC 19 December 2010, e) 0000 UTC 19 December 2010, d) 1800 UTC 18 December 2010, c) 1200 UTC 18 December 2010, b) 0000 UTC 18 December 2010 and a) not data available due to forecast length. Return to text.

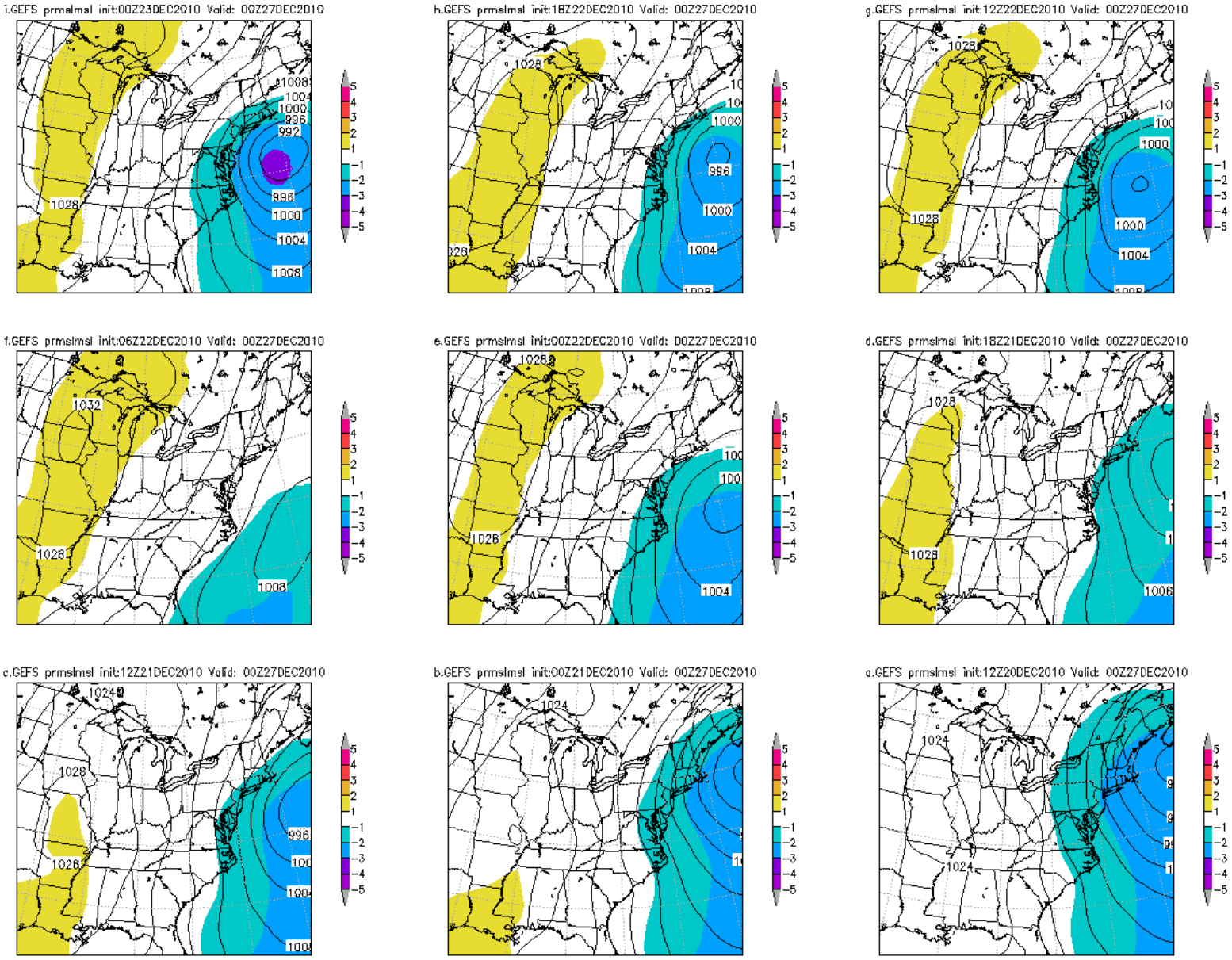

Figure 10. As in Figure 9 except for forecast valid at 0000 UTC 27 December 2010 initialized at i) 0000 UTC 23 December 2010, h) 1800 UTC 22 December 2010, g) 1200 UTC 22 December 2010, f) 0600 UTC 22 December 2010, e) 0000 UTC 22 December 2010, d) 1800 UTC 21 December 2010, c) 1200 UTC 21 December 2010, b) 0000 UTC 21 December 2010 and a) 1200 UTC 20 December 2010. Return to text.

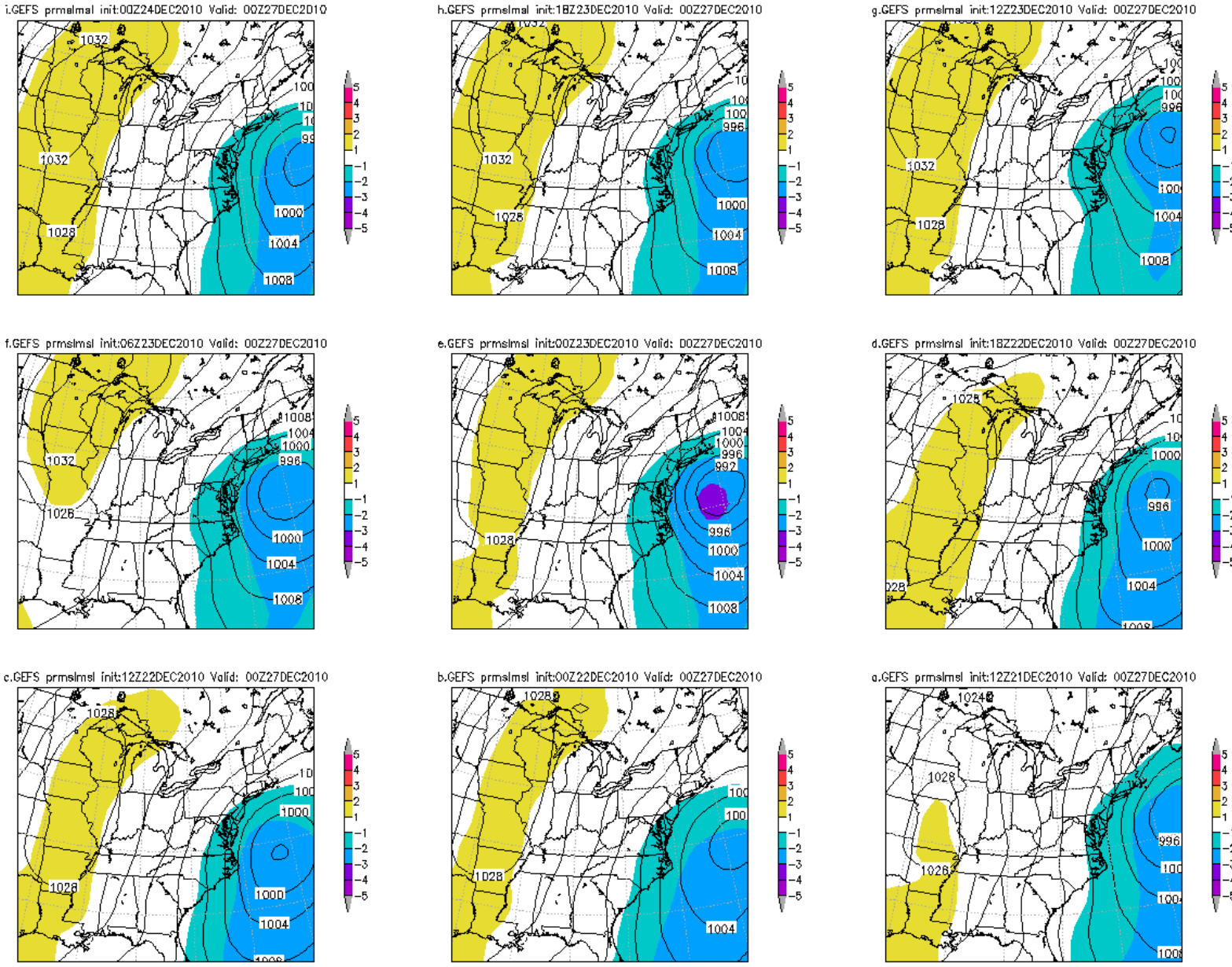

Figure 11. As in Figure 9 except for GEFS ensemble mean valid at 0000 UTC 27 December 2010 from forecasts initialized at i) 0000 UTC 24 December 2010, h) 1800 UTC 23 December 2010, g) 1200 UTC 23 December 2010, f) 0600 UTC 23 December 2010, e) 0000 UTC 23 December 2010, d) 1800 UTC 22 December 2010, c) 1200 UTC 22 December 2010, b) 0000 UTC 22 December 2010 and a) 1200 UTC 21 December 2010. Return to text.

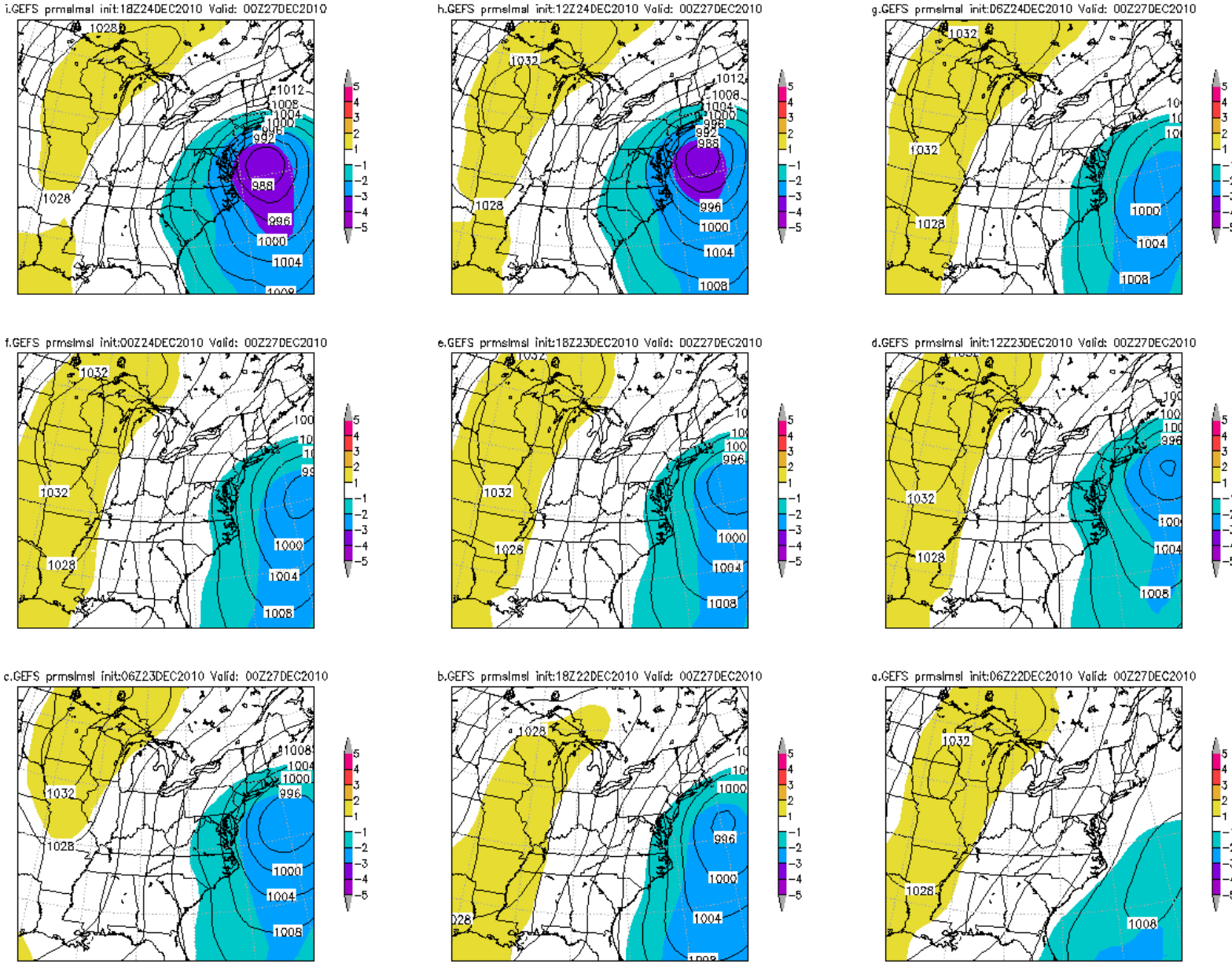

Figure 12. As in Figure 9 except for the GEFS initialized at i) 1800 UTC 24 December 2010, h) 1200 UTC 24 December 2010, g) 0600 UTC 24 December 2010, f) 0000 UTC 24 December 2010, e) 1800 UTC 23 December 2010, d) 1200 UTC 23 December 2010, c) 0600 UTC 23 December 2010 b)1800 UTC 23 December 2010 and a) 0600 UTC 23 December 2010. Return to text.

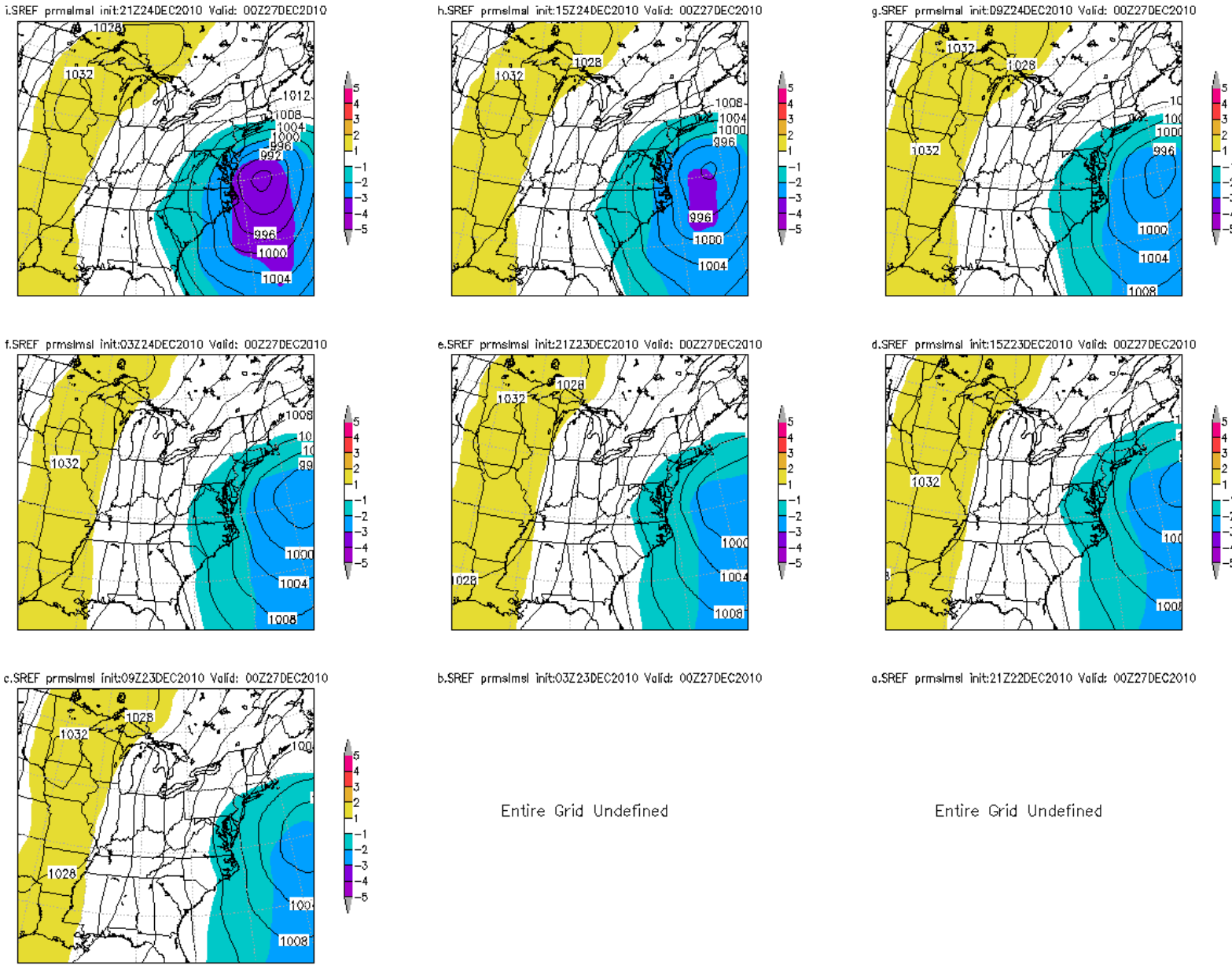

Figure 13. As in Figure 12 except for NCEP SREF forecasts valid at 0000 UTC 27 December 2010 from forecasts initialized at Return to text.

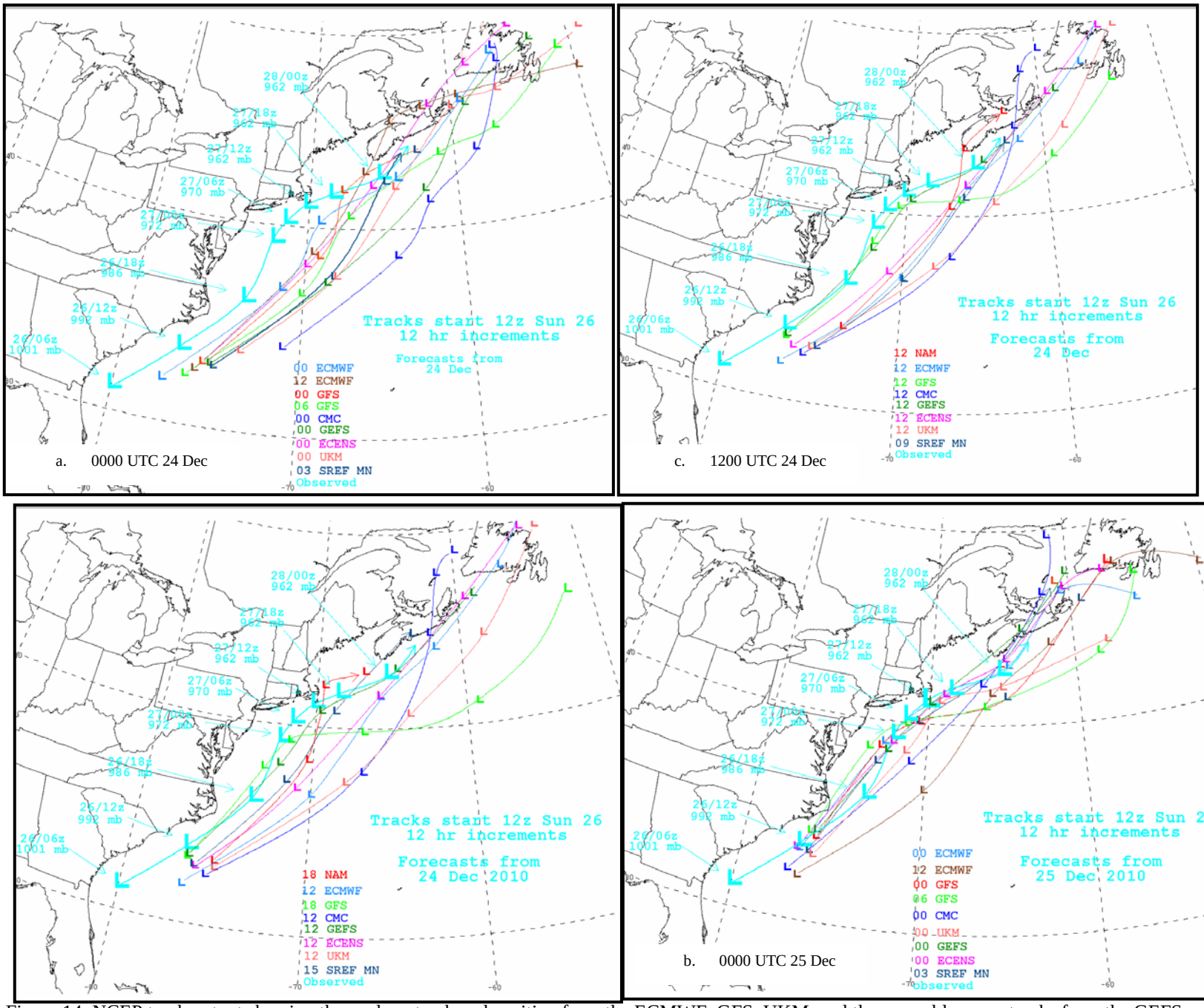

Figure 14. NCEP track output showing the cyclone track and position from the ECMWF, GFS, UKM, and the ensemble mean tracks from the GEFS, ECWMF ensemble and the SREF. The cyan color shows the verifying analysis with time and pressure values. Members are color coded in each figure f cycle time. Panels are a) 24 December 0000 UTC cycles, b) 24 1200 UTC cycles, c) 24 1800 UTC cycles, and d) 25 0000 UTC cycles. The SREF cycle are off by 3 hours showing the next SREF run after the time in the panel. Some panels show 2 EC runs. Return to text.

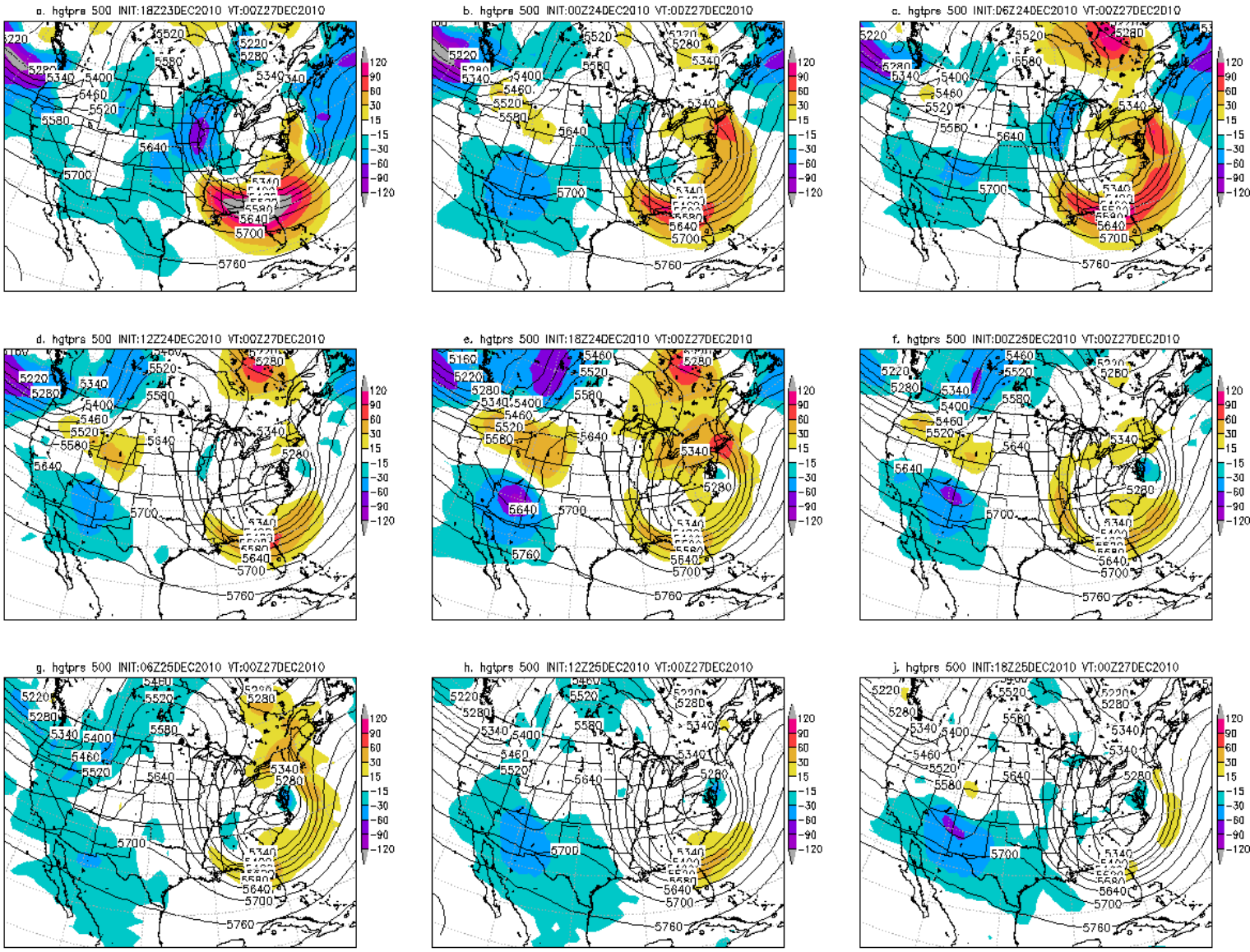

Figure 15. GFS heights (m) and height errors valid at 0000 UTC 27 December 2010 from GFS forecast initialized at a) 1800 UTC 23 December, b) 0000 UTC 24 December c) 0600 UTC 24 December, d) 1200 UTC 24 December, e) 1800 UTC 24 December, f) 0000 UTC 25 December, g) 0600 UTC 25 December, h) 1200 UTC 25 December and i) 1800 UTC 25 December 2010. The 00-hour GFS analysis was used as verification and errors are computed as forecast minus observed. Return to text.

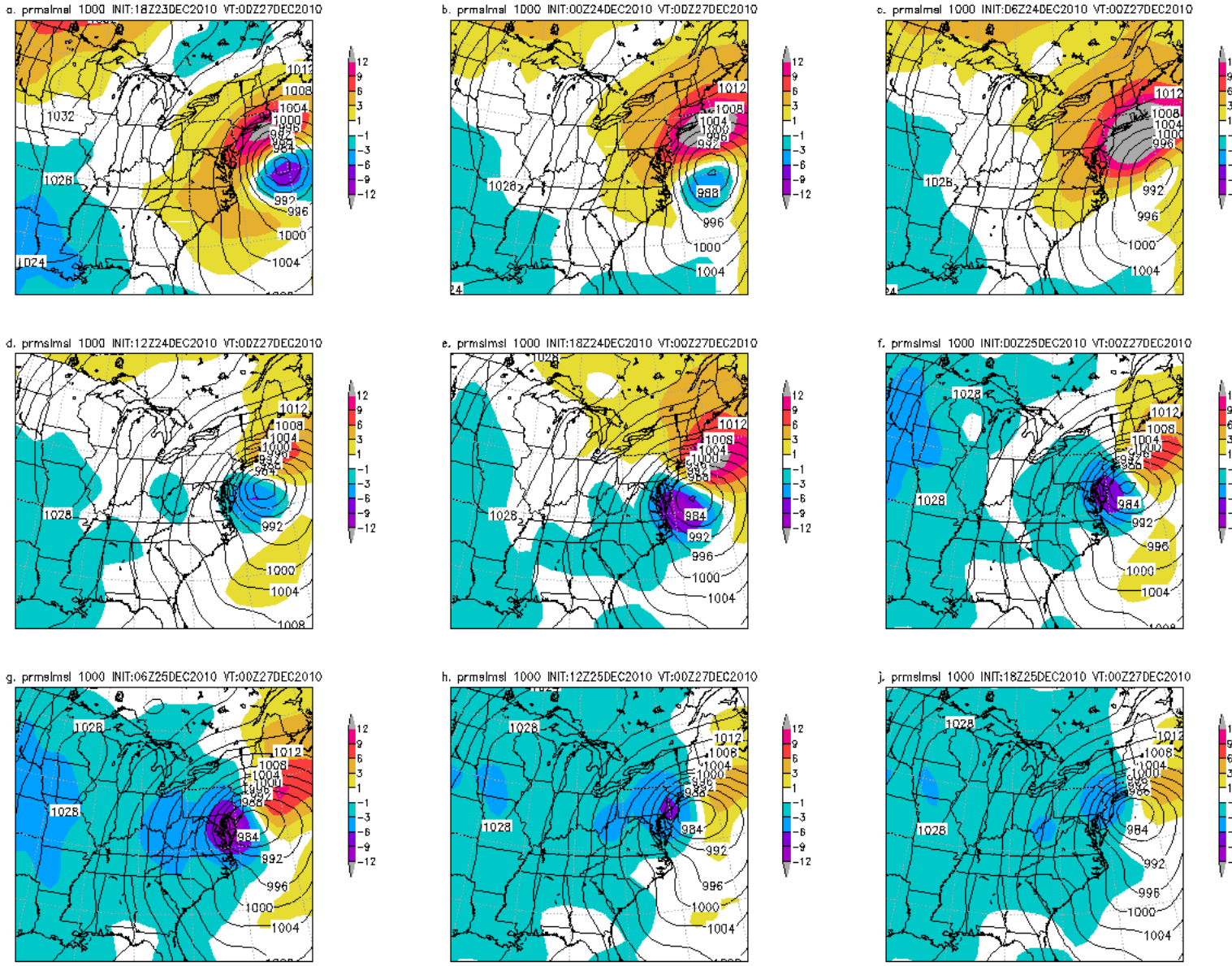

Figure 16. As in Figure 15 except for GFS forecasts of mean sea level pressure (hPa) and pressure errors (hPa). Return to text.

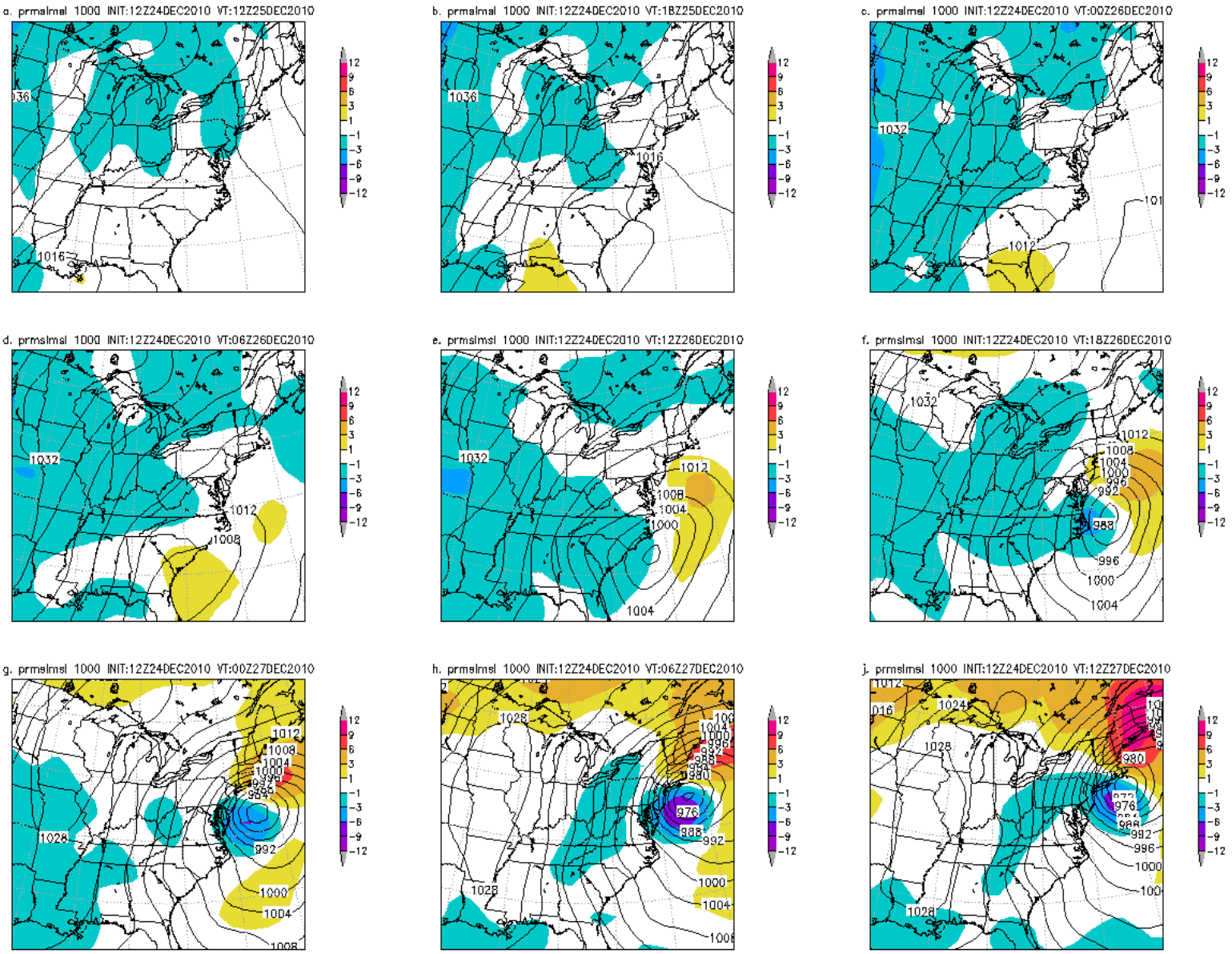

Figure 17. As in Figure 16 except for the GFS initialized at 1200 UTC 24 December 2010 showing forecasts valid at a) 1200 UTC 25 December, b) 1800 UTC 25 December, c) 0000 UTC 26 December, d) 0600 UTC 26 December, e) 1200 UTC 26 December, f) 1800 UTC 26 December, g) 0000 UTC 27 December, h) 0600 UTC 27 December and i) 1200 UTC 27 December 2010. Return to text.

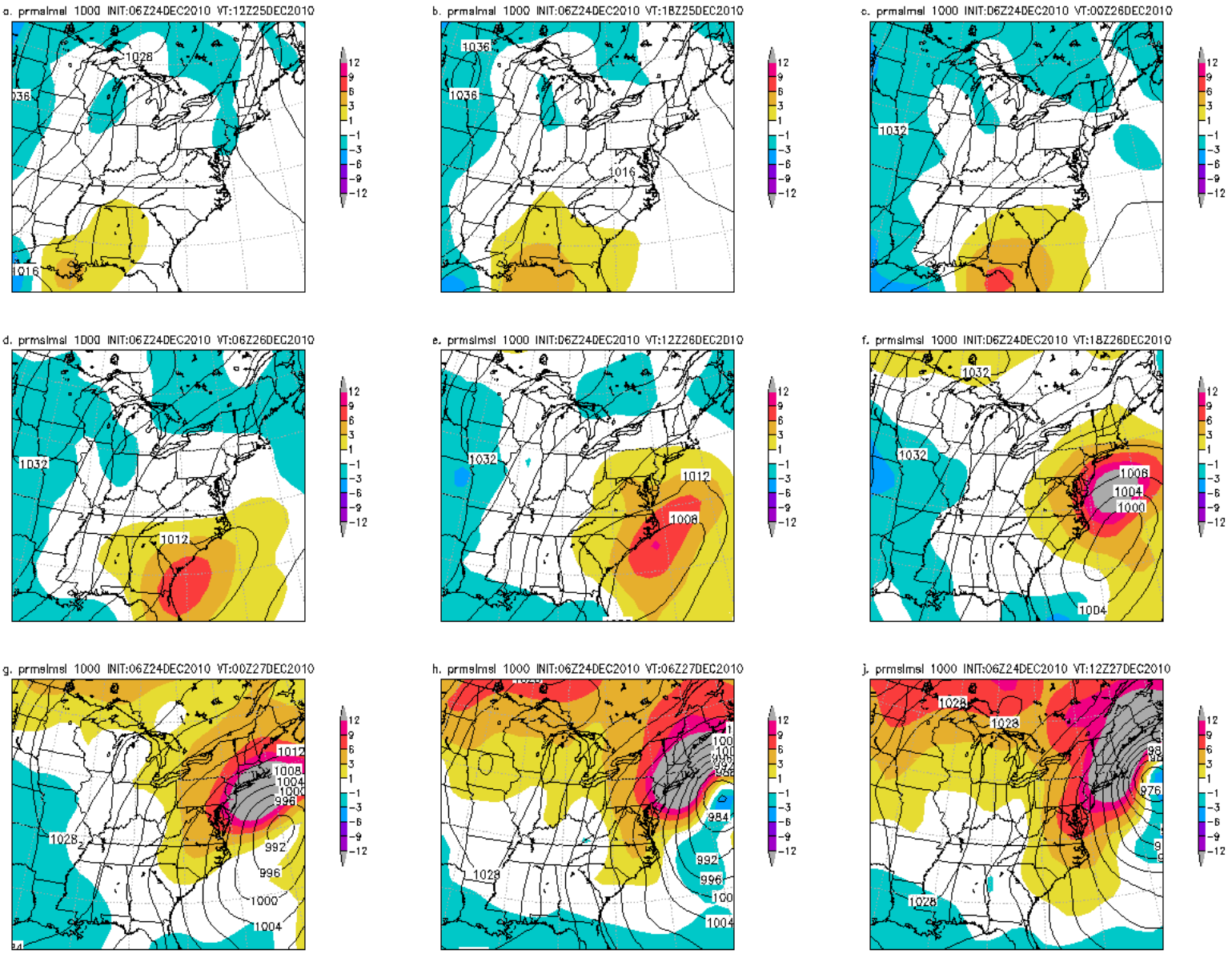

Figure 18. As in Figure 17 except for GFS initialized at 0600 UTC 24 December 2010. Return to text.

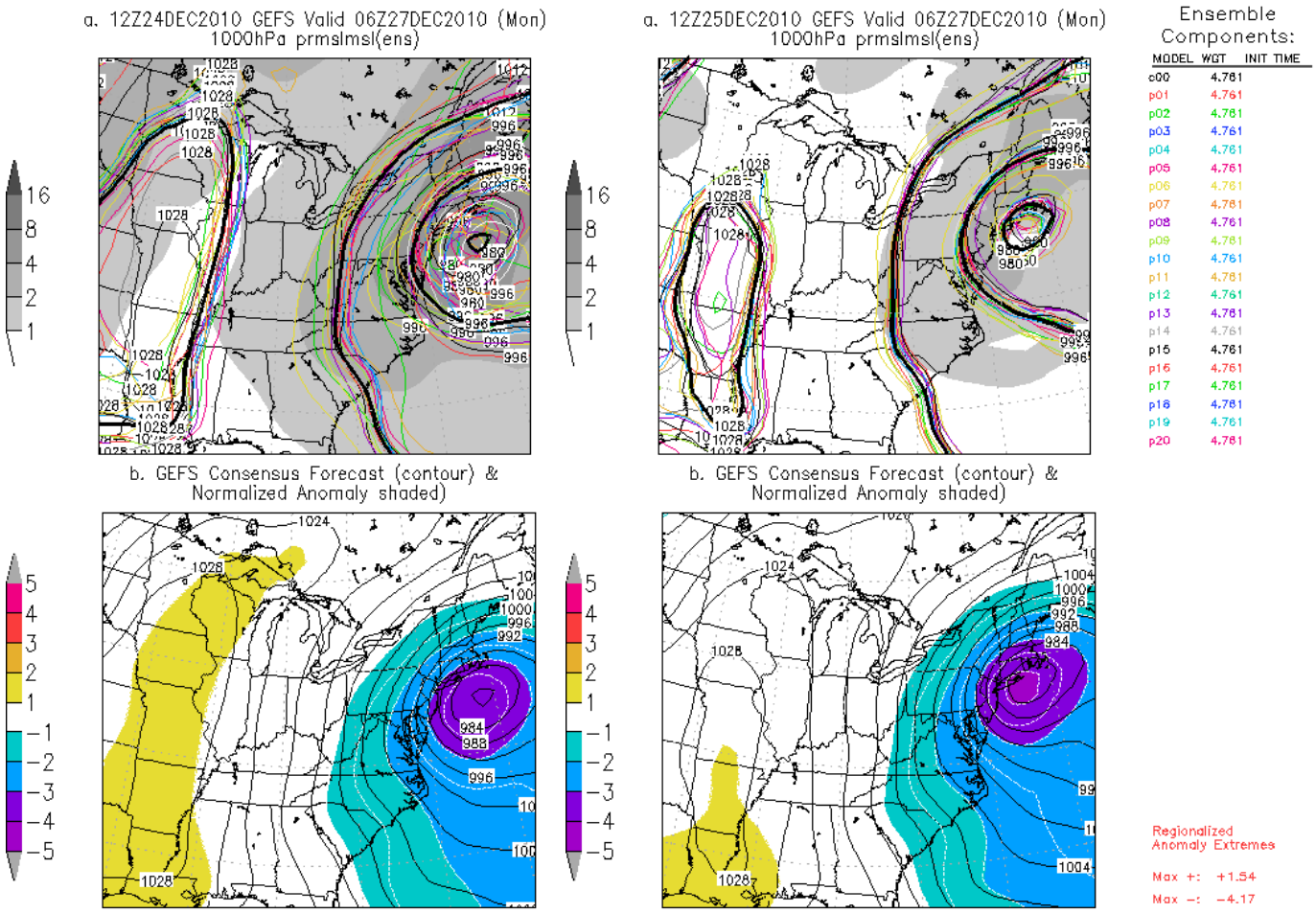

Figure 19. GEFS forecasts initialized at (left) 1200 UTC 24 December and (right) 25 December 2010. Upper panels show the spaghetti plots and the spread in the GEFS with the 996, 1008 and 1028 hPa contours shown. Lower panels show the ensemble mean values and the standardized anomalies of these forecasts. Return to text.